ON 4-MANIFOLDS, FOLDS AND CUSPS

STEFAN BEHRENS

Abstract. We study *simple wrinkled fibrations*, a variation of the simplified purely wrinkled fibrations introduced in [W1], and their combinatorial description in terms of *surface diagrams*. We show that simple wrinkled fibrations induce handle decompositions on their total spaces which are very similar to those obtained from Lefschetz fibrations. The handle decompositions turn out to be closely related to surface diagrams and we use this relationship to interpret some cut-and-paste operations on 4-manifolds in terms of surface diagrams. This, in turn, allows us classify all closed 4-manifolds which admit simple wrinkled fibrations of genus one, the lowest possible fiber genus.

1. Introduction

After the pioneering work of Donaldson and Gompf on symplectic manifolds and Lefschetz fibrations [D, GS] (and later Auroux, Donaldson and Katzarkov on near-symplectic manifolds [ADK]), the study of singular fibration structures on smooth 4-manifolds has drawn a considerable interest among 4-manifold theorists. Among the highlights in the field have been existence results for so called *broken Lefschetz fibrations* over the 2-sphere on all closed, oriented 4-manifolds [AK, B1, GK1, L] as well as a classification of these maps up to homotopy [L, W1]. Furthermore, the classical observation that Lefschetz fibrations over the 2-sphere are accessible via handlebody theory and can be described more or less combinatorially in terms of collections of simple closed curves on a regular fiber known as the *vanishing cycles* [K, GS] was extended to the broken Lefschetz setting in [B2].

Our starting point is the work of Williams [W1] who introduced the closely related notion of *simplified purely wrinkled fibrations*, proved their existence and exhibited a similar combinatorial description of these maps, again by collections of simple closed curves on a regular fiber, which he calls *surface diagrams*. In particular, it follows that all smooth, closed, oriented 4-manifolds can be described by a surface diagram. However, the correspondence between simplified purely wrinkled fibrations and surface diagrams has been somewhat unsatisfactory in that it usually involves arguments using broken Lefschetz fibrations and one has to assume the fiber genus to be sufficiently high.

It is one of our goals to provide a detailed and intrinsic account of this correspondence and to clarify the situation in the lower genus cases. After that we will give some applications. Let us describe the contents of this paper in more detail.

We begin by recalling some preliminaries from the singularity theory of smooth maps and the theory of mapping class groups of surfaces. This section is slightly lengthy because we intend to use it as a reference for future work.

The following two sections form the technical core of this paper. In Section 3 we introduce *simple wrinkled fibrations* over a general base surface. In the case when the base is the 2-sphere our definition is almost equivalent to Williams' simplified purely wrinkled fibrations and our reason for introducing a new name is mainly to

Date: May 22, 2012.

Key words and phrases. 4-manifolds, fold, cusp, simplified purely wrinkled fibration, broken Lefschetz fibration, surface diagram.

reduce the number of syllables. We then explain how the study of simple wrinkled fibrations reduces to certain fibrations over the annulus which we call *annular simple wrinkled fibrations*. From these we extract *twisted surface diagram* and establish a correspondence between annular simple wrinkled fibrations and twisted surface diagrams (Theorem 3.15) up to suitable notions of equivalence. Along the way we show that annular simple wrinkled fibrations induce (relative) handle decompositions of their total spaces which are, in fact, encoded in a twisted surface diagram (Section 3.2). These handle decompositions bare a very close resemblance with those obtained from Lefschetz fibrations, the only difference appearing in the framings of certain 2-handles. The section ends with an investigation of the ambiguities for gluing surface bundles to the boundary components of annular simple wrinkled fibrations.

In Section 4 we specialize to the case when the base surface is either the disk or the 2-sphere and recover Williams' setting. Using our results about annular simple wrinkled fibrations we obtain a precise correspondence between Williams' (untwisted) surface diagrams and certain simple wrinkled fibrations over the disk (Proposition 4.1). In particular, our approach provides a direct way to construct a simple wrinkled fibration from a given surface diagram circumventing the previously necessary detour via broken Lefschetz fibrations.[1]

Next, we address the question which surface diagrams describe simple wrinkled fibrations that extend to fibrations over the sphere and thus describe closed 4-manifolds. Just as in the theory of Lefschetz fibrations the key is to understand the boundary of the associated simple wrinkled fibration over the disk. We show how to identify this boundary with a mapping torus and describe its monodromy in terms of the surface diagram. Unfortunately, it turns out that the boundary is much harder to understand than in the Lefschetz setting.

We then go on to review the handle decompositions exhibited in Section 3 when the base is the disk or the sphere and describe a recipe for drawing Kirby diagrams for them. To complete the picture, we compare our decompositions with the ones obtained via simplified broken Lefschetz fibrations.

In the Sections 5 and 6 we give some applications. We show that certain substitutions of curve configurations in surface diagrams correspond to cut-and-paste operations on 4-manifolds. In particular, we give a surface diagram interpretation of blow-ups and sum-stabilizations, i.e. connected sums with $\mathbb{C}P^2$, $\overline{\mathbb{C}P^2}$ and $S^2 \times S^2$. Using these we easily obtain a classification of closed 4-manifolds which admit simple wrinkled fibrations with the lowest possible fiber genus.

Theorem 1.1. *A smooth, closed, oriented 4-manifold admits a simple wrinkled fibration of genus one if and only if it is diffeomorphic to* $kS^2 \times S^2$ *or* $m\mathbb{C}P^2 \# n\overline{\mathbb{C}P^2}$ *where* $k, m, n \geq 1$.

This result should be compared to [BK] and [H1] where a classification of genus one simplified broken Lefschetz fibration is addressed but only partially achieved. However, it should also be noted that the latter class of maps is strictly larger than that of genus one simple wrinkled fibrations and it is thus conceivable that the classification is more complicated.

In the final Section 7 we close this paper with some remarks highlighting some major problems in the field and outline some related developments.

Conventions. By default all manifolds are smooth, compact and orientable and all diffeomorphisms are orientation preserving. When we speak of neighborhoods

[1] By now this can be considered as a special case of [GK4] which appeared while we were writing this paper.

of submanifolds we always mean tubular neighborhoods. We use the symbol νS (resp. $\bar{\nu} S$) for an open (resp. closed) tubular neighborhood of a submanifold $S \subset M$.

For induced orientations on boundaries we use the *outward normal first* convention. Moreover, if $f\colon M \to N$ is smooth, M and N are connected and $p \in N$ is a regular value, then orientations on two out of the three manifolds M, N and $f^{-1}(p)$ induce an orientation on the third as follows. There is a small ball $D \subset N$ containing p such that $f^{-1}(D)$ can naturally be identified with $f^{-1}(p) \times D$ and we choose the third orientation such that this identification preserves orientations where $f^{-1}(p) \times D$ carries the product orientation.

Finally, (co-)homology is always taken with integral coefficients. Exceptions to these rules will be explicitly stated and we reserve the right to sometimes restate some of the conditions for emphasis.

Acknowledgements. This work is part of the author's ongoing PhD project carried out at the Max-Planck-Institute for Mathematics in Bonn, Germany. The author would like to thank Inanc Baykur for helpful comments on an early draft of this paper as well as his advisor Prof. Dr. Peter Teichner for letting him work on this project.

2. Preliminaries

To fix some terminology, let $f\colon M \to N$ be a smooth map with differential $df\colon TM \to TN$. A *critical point* (or a *singularity*) of f is a point $p \in M$ such that df_p is not surjective. The set of critical points, called the *critical locus* of f, will be denoted by

$$\mathcal{C}_f := \{p \in M | \operatorname{rk} df_p < \dim N\} \subset M.$$

The image of a critical point is called a *critical value* and the set of all critical values is called the *critical image* of f.

As customary, we will call the preimage of a point a *fiber*, usually decorated with the adjectives regular or singular indicating whether or not the fiber contains critical points. Note that regular fibers are always smooth submanifolds with trivial normal bundle.

2.1. Folds, cusps and Lefschetz singularities.

As a warm up, recall that a generic map from any compact manifold to a 1-dimensional manifold has only finitely many critical points on which it is injective and, moreover, all critical points are of *Morse type*, i.e. they are locally modeled[2] on the maps

$$(x_1, \dots, x_n) \mapsto -x_1^2 - \dots - x_k^2 + x_{k+1}^2 + \dots + x_n^2,$$

where the number k is called the *(Morse) index* of the critical point.

A similar statement holds for maps to surfaces. For convenience we will take the source to be 4-dimensional from now on. In this setting the Morse critical points are replaced by two types of singularities known as *folds* and *cusps* which can also be described in terms of local models. The model for a fold singularity is the map $\mathbb{R}^4 \to \mathbb{R}^2$ given by the formula

$$(t, x, y, z) \mapsto (t, -x^2 - y^2 \pm z^2) \tag{2.1}$$

and the cusps are locally modeled on

$$(t, x, y, z) \mapsto (t, -x^3 + 3tx - y^2 \pm z^2). \tag{2.2}$$

[2]A map $f\colon M^m \to N^n$ is *locally modeled around* $p \in M$ on $f_0\colon : \mathbb{R}^m \to \mathbb{R}^n$ if there are local coordinates around p and $f(p)$ mapping these points to the origin such that the coordinate representation of f agrees with f_0.

If the sign in either of the above equations is positive (resp. negative), then the singularity is called *indefinite* (resp. *definite*).

An easy calculation shows that the critical loci of the fold and cusp models are given by $\{\,(r,0,0,0) \mid r \in \mathbb{R}\,\}$ and $\left\{\,(r^2,r,0,0) \;\middle|\; r \in \mathbb{R}\,\right\}$, respectively. As a consequence, the critical image of a smooth map is a smooth 1-dimensional submanifold near fold and cusp points. The critical images of both models are shown in Figure 2.1. Note that the critical image is smoothly embedded in the fold model where

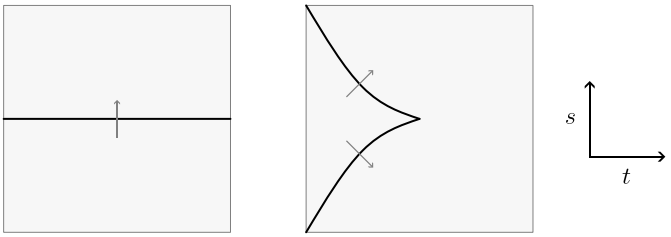

FIGURE 1. The critical images of the fold and cusp models.

as in the cusp case it is topologically embedded via a smooth homeomorphism whose inverse fails to be smooth only at the cusp point.

It follows directly from the models that folds always come in 1-dimensional families on which the map restricts to an immersion. We will usually be sloppy and refer to such an arc of fold points in the source as well as their image in the target as *fold arcs*. Furthermore, cusps are isolated in the critical locus in the sense that there is a small neighborhood which contains no other cusps. However, cusps are not isolated singularities. In fact, one can show that any cusp is surrounded by two fold arcs, at least one of which is indefinite.

We can now state the normal form of generic maps from 4-manifolds to surfaces.

Theorem 2.1 (Normal form of maps to surfaces)**.** *A generic map from a 4-manifold to a surface has only fold and cusp singularities, it is injective on the cusps and restricts to an immersion with only transverse intersections between fold arcs.*

Note, in particular, that the above discussion shows that the critical locus of a generic map to a surface is a smooth 1-dimensional submanifold of the source. For more details, including a proof of the above theorem for arbitrary source dimension, we refer the reader to [GG].

Remark 2.2. Recently, these generic maps to surfaces have appeared under the name *Morse 2-functions* in the work of Gay and Kirby [GK2, GK3, GK4].

In what follows we will only deal with indefinite singularities. So from now on, when we speak of folds and cusps, we will always mean the indefinite ones.

Figure 2.1 contains some further decorations which we will now explain. Both, the fold and the cusp singularity are intimately related to 3-dimensional Morse-Cerf theory. The fold models a trivial homotopy of a Morse functions with one critical point (of index two) on the vertical slices. This means that the model restricted to a small arc transverse to the fold locus is a Morse function with one critical point of index one or two depending on the direction. The arrows in the picture indicate the direction in which the index is two. Note that the topology of the fibers of either side of a fold arc is necessarily different.

Similarly, the cusp is also a homotopy of Morse functions on the vertical slices, although a nontrivial one. It models the cancellation of a pair of critical points (of index one and two). The arrows indicate the index two direction of the fold arcs adjacent to the cusp.

For the moment, this is all we have to say about folds and cusps. Another important type of singularity which has its roots in (complex) algebraic geometry is the *Lefschetz singularity* and its local model is given in complex coordinates by

$$L\colon \mathbb{C}^2 \to \mathbb{C} \quad ; \quad (z,w) \mapsto zw.$$

At this point it becomes important whether the charts that we use to model the map are orientation preserving. Although this does not matter for folds and cusps[3], it makes a surprisingly big difference in the case of Lefschetz singularities. So from now on we will always use orientation preserving charts to model singularities whenever the source or target are oriented.

As stated in the introduction, maps with (indefinite) fold, cusp and Lefschetz singularities have been prominently featured in many research papers over the past decade. Unfortunately, various authors have used various names for various types of maps and there is yet no commonly accepted terminology in the field. For the purpose of this paper we will use the following terminology.

Definition 2.3. A surjective map $f\colon X \to B$ from an oriented 4-manifold to an oriented surface is called (a) a *wrinkled fibration*, (b) a *(broken) Lefschetz fibration* or (c) a *broken fibration* if its critical locus contains only

(a) indefinite folds and cusps,
(b) Lefschetz singularities (and indefinite folds),
(c) indefinite folds, cusps and Lefschetz singularities,

all critical points are contained in the interior of X and all intersections in the critical image are transverse intersections of fold arcs.

In accordance with the use of the word fibration we will usually refer to the source as the *total space* and to the target as the *base*. Note that the regular fibers of a broken fibration are (orientable) surfaces. Furthermore, if we assume that $\partial X = f^{-1}(\partial B)$, which we will do later on, then the fibers are closed.

It is quite useful to think of broken fibrations as (singular) families of surfaces parametrized by the base. More precisely, the images of the folds and cusps cut the base into several regions which may or may not contain Lefschetz singularities. The regular fibers are (orientable) surfaces whose topological type depends only on the region that it maps into. One thus decorates the base with the topological type of the fibers over each region together with some information about what happens to a fiber if one crosses a fold arc (the little arrows we have indicated above together with the corresponding fold vanishing cycle) or runs into a Lefschetz singularity (the Lefschetz vanishing cycle). Under certain circumstances this data is enough to determine the map as we will see later on (see also [GK4]).

We finish this section with a short review of the homotopy classification of broken fibrations over S^2 that was mentioned in the introduction. An important contribution of Lekili [L] is that he showed how to pass back and forth between broken Lefschetz fibrations and wrinkled fibrations via two *local homotopies*, i.e. homotopies that are supported in arbitrarily small balls. As portrayed in Figure 2 one can *wrinkle* a Lefschetz point into an indefinite triangle (i.e. an indefinite circle with three cusps) and one can exchange a cusp for a Lefschetz singularity, this move is sometimes called *unsinking* a Lefschetz point from a fold. (Moreover, he showed that these modifications work equally well with achiral Lefschetz singularities which, together with the results of [GK1], proves the existence of broken Lefschetz fibrations.) As a consequence, one can translate questions about broken fibrations into questions about wrinkled fibrations which are accessible by means

[3]For both models there are orientation reversing diffeomorphisms which leave the map invariant

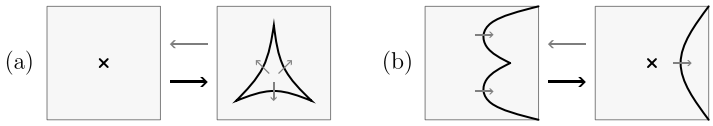

FIGURE 2. (a) Wrinkling and (b) unsinking a Lefschetz singularity.

of singularity theory. For example, there is a structural result similar to Theorem 2.1 for generic homotopies between wrinkled fibrations. The basic building blocks include isotopies of the base and total space and three types of modifications (and their inverses) that are realized by local homotopies: the *birth/death*, the *merge* and the *flip*. Figure 3 shows their effect on the critical image. In gen-

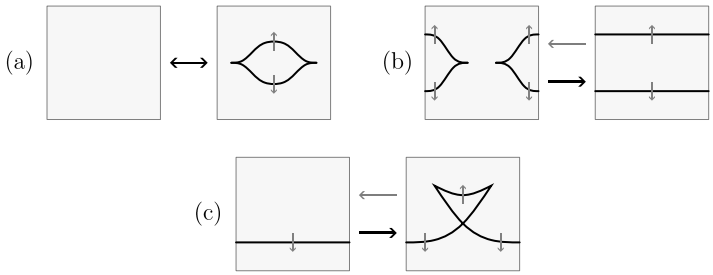

FIGURE 3. The basic local homotopies: (a) birth, (b) merge, (c) flip.

eral, such a generic homotopy will pass through maps with definite singularities. However, the main theorem in [W1] states that indefinite singularities can, in fact, be avoided. In other words, any two homotopic wrinkled fibrations are homotopic through wrinkled fibrations.

Remark 2.4. It has become common to refer to an application of any of the above mentioned modifications as *moves* performed on a broken fibration. It is important to note that most of these moves are not strictly reversible in the following sense. If the critical image of a given broken fibration exhibits a configuration as on the left hand side of any of the pictures, then it is always possible to replace it by the configuration on the right hand side. However, it might not be possible to go into the other direction. The only exception is the birth. In all other cases some extra conditions are needed to go from right to left. This is indicated in our pictures with shaded arrows.

Remark 2.5. There has been some disagreement in the literature about which direction in Figure 3(b) should be called merge and which inverse merge. To avoid this decision we will simply speak of *merging cusps* and *merging folds*, respectively.

2.2. **Surfaces and simple closed curves.** As we pointed out, the regular fibers of broken fibrations are surfaces and these fibers will be prominently featured later on. Unfortunately, this is yet another field of mathematics in which different authors use different conventions and, in the current author's experience, it can be confusing to decide whether a statement in some reference actually applies to a situation at hand. For that reason we will give very precise definitions, deliberately risking to be overly precise.

By a *surface* Σ we mean a compact, orientable, 2-dimensional manifold, possibly with boundary and some marked points in the interior. A *simple closed curve* in Σ is a closed, connected, 1-dimensional submanifold of Σ that does not meet

the boundary or the marked points. We usually consider simple closed curves up to ambient isotopy in Σ relative to $\partial\Sigma$ and the marked points and will not make a notational distinction between a simple closed curve and its isotopy class. Note that according our definition simple closed curves are unoriented objects. However, from time to time it will be convenient to choose orientations on them in order to speak of their homology classes.

Given two simple closed curves $a, b \subset \Sigma$ we define their *geometric intersection number* as

$$i(a,b) := \min\{\#(\alpha \cap \beta) | \alpha \sim a,\ \beta \sim b,\ \alpha \pitchfork \beta\} \in \mathbb{N}$$

where the signs $\sim$ and $\pitchfork$ indicate isotopy and transverse intersection. If the curves as well as the surface are oriented, then we also have an *algebraic intersection number* which is obtained by a signed count of intersections after making the curves transverse. Equivalently, this number can be described as

$$\langle a, b\rangle := \langle [a], [b]\rangle_\Sigma := \langle [a], [b]\rangle_{H_1(\Sigma)} \in \mathbb{Z}$$

where bracket on the right hand side denotes the intersection form on $H_1(\Sigma)$.

Note that the algebraic intersection number is alternating and depends only on the homology classes of the oriented simple closed curves while the geometric intersection number is symmetric and depends on the isotopy classes. Both intersection numbers have the same parity (i.e. even or odd) and satisfy the inequality

$$|\langle a, b\rangle| \leq i(a,b). \tag{2.3}$$

We say that a and b are *geometrically dual* (resp. *algebraically dual*) if their geometric (reap. algebraic) intersection number is one.

A simple closed curve $a \subset \Sigma$ is called *non-separating* if its complement is connected, otherwise it is called *separating*. Note that a simple closed curve is separating if and only if it is null-homologous (with either orientation) and thus simple closed curves that have geometric or algebraic duals are automatically non-separating.

2.2.1. *Diffeomorphisms of surfaces.* Let us now turn to diffeomorphisms of surfaces. Let $\mathrm{Diff}^+(\Sigma, \partial\Sigma)$ denote the set of orientation preserving diffeomorphisms that restrict to the identity on $\partial\Sigma$ and preserve the set of marked points. The *mapping class group* of Σ is defined as

$$\mathcal{M}(\Sigma) := \pi_0(\mathrm{Diff}^+(\Sigma, \partial\Sigma), \mathrm{id}).$$

Given a simple closed curve $a \subset \Sigma$ there is a well defined mapping class $\tau_a \in \mathcal{M}(\Sigma)$ called the (right-handed) *Dehn twist* about a. Similarly, any simple arc $r \subset \Sigma$ that connects two distinct marked points gives rise to a *half twist* $\bar{\tau}_r \in \mathcal{M}(\Sigma)$.

It is well known that $\mathcal{M}(\Sigma)$ is generated by the collection of Dehn twist and half twists, where the latter are only needed in the presence of marked points. On the other hand, mapping classes can be effectively studied by their action on (isotopy classes of) simple closed curves. In particular, it is desirable to understand the effect of Dehn twists on simple closed curves. While this can be tricky, the situation simplifies significantly on the level of homology classes.

Proposition 2.6 (Picard-Lefschetz formula)**.** *Let Σ be a surface, $a \subset \Sigma$ a simple closed curve and let $x \in H_1(\Sigma)$. Then for any orientation on a we have*

$$(\tau_a^k)_* x = x + k\,\langle [a], x\rangle\,[a]. \tag{2.4}$$

In particular, if b is an oriented simple closed curve, then

$$[\tau_a^k(b)] = [b] + k\,\langle [a], [b]\rangle\,[a]. \tag{2.5}$$

Proof. See [FM], Proposition 6.3. □

Remark 2.7. The Picard-Lefschetz formula is particularly useful for the torus since, in that case, mapping classes are completely determined by their action on homology.

Another useful tool is the so called *change of coordinates principle* which roughly states that any two configurations of simple closed curves on a surface with the same intersection pattern can be mapped onto each other by a diffeomorphism. We will only use the following special cases. For details we refer to [FM], Chapter 1.3.

Proposition 2.8 (Change of coordinates principle)**.** *If $a, b \subset \Sigma$ is a pair of non-separating simple closed curves, then there exists some $\phi \in \mathrm{Diff}^+(\Sigma, \partial\Sigma)$ such that $\phi(a) = b$. Furthermore, if a, b and a', b' are two pairs of geometrically dual curves, then there is some $\phi \in \mathrm{Diff}^+(\Sigma, \partial\Sigma)$ such that $\phi(a) = a'$ and $\phi(b) = b'$.*

2.2.2. *Mapping tori and their automorphisms.* Given a surface Σ and a diffeomorphism $\mu\colon \Sigma \to \Sigma$ we can form its *mapping torus*

$$\Sigma(\mu) := \big(\Sigma \times [0,1]\big)/\big((x,1) \sim (\mu(x),0)\big)$$

which is a 3-manifolds that carries a canonical map to $S^1 \cong [0,1]/\{0,1\}$ which turns out to be a submersion. In other words, $\Sigma(\mu)$ fibers over S^1. If Σ is oriented and μ is orientation preserving, then our conventions in the introduction induce an orientation on $\Sigma(\mu)$. It is well known that all surface bundles over S^1 can be described as mapping tori. Indeed, if a 3-manifold fibers over S^1, then one chooses a fiber and a lift of a vector field that determines the orientation of S^1 and the return map of the flow of this vector field induces a diffeomorphism of the fiber which is usually called the *monodromy*.

Let Y be an oriented 3-manifold that fibers over the circle via a map $f\colon Y \to S^1$. An *automorphism* of (Y, f) is an orientation and fiber preserving diffeomorphism of Y. We denote the group of automorphisms by $\mathrm{Aut}(Y, f)$ or simply by $\mathrm{Aut}(Y)$ when the fibration is clear from the context. If we identify Y with a mapping torus, say $\Sigma(\mu)$, then we obtain a description of $\mathrm{Aut}(Y)$ in terms of diffeomorphisms of Σ. Indeed, any element $\phi \in \mathrm{Aut}(\Sigma(\mu))$ can be considered as a path $(\phi_t)_{t\in[0,1]}$ in $\mathrm{Diff}^+(\Sigma)$ connecting some element $\phi_0 \in \mathrm{Diff}^+(\Sigma)$ to $\phi_1 = \mu^{-1}\phi_0\mu$. In particular, ϕ_0 must be isotopic to $\mu^{-1}\phi_0\mu$ and thus represents an element of $C_{\mathcal{M}(\Sigma)}(\mu)$, the centralizer in $\mathcal{M}(\Sigma)$ of (the mapping class represented by) μ. Elaborating on this idea one arrives at the conclusion that

$$\pi_0\big(\mathrm{Aut}(Y)\big) \cong \pi_0\big(\mathrm{Aut}(\Sigma(\mu))\big) \cong C_{\mathcal{M}(\Sigma)}(\mu) \ltimes \pi_1(\mathrm{Diff}(\Sigma), \mathrm{id}), \tag{2.6}$$

where the multiplication on the right hand side is given by

$$(g, \sigma) \cdot (h, \tau) = (h \circ g, (g^{-1}\tau g) * \sigma).$$

This means that there are essentially two types of automorphism of mapping tori, the ones that are constant on the fibers coming from $C_{\mathcal{M}(\Sigma)}(\mu)$ and the ones coming from $\pi_1(\mathrm{Diff}(\Sigma), \mathrm{id})$ that vary with the fibers and restrict to the identity on the reference fiber. Fortunately, there are no non-constant automorphisms most of the time due to the following classical result.

Theorem 2.9 (Earle-Eells, [EE])**.** *Let Σ be a closed, orientable surface of genus g without marked points. Then*

$$\pi_1(\mathrm{Diff}(\Sigma), \mathrm{id}) \cong \begin{cases} \mathbb{Z}_2 & \text{if } g = 0 \\ \mathbb{Z} \oplus \mathbb{Z} & \text{if } g = 1 \\ 1 & \text{if } g \geq 2. \end{cases}$$

Hence, as soon as the genus of the fiber of a mapping torus is at least two, all automorphisms are isotopic (through automorphisms) to constant ones.

Remark 2.10. It is important not to confuse the group $\mathrm{Aut}(Y)$ with the group of all (orientation preserving) diffeomorphisms of Y. A general diffeomorphism will not even be isotopic to a fiber preserving one!

Theorem 2.9 has many important consequences of which we only highlight one.

Corollary 2.11. *Let $P \to S^2$ be a surface bundle with closed fibers of genus g.*

1. *If $g = 0$, then P is diffeomorphic to $S^2 \times S^2$ or $\mathbb{C}P^2 \# \overline{\mathbb{C}P^2}$.*
2. *If $g = 1$, then P is diffeomorphic to $T^2 \times S^2$, $S^1 \times S^3$ or $S^1 \times L(n, 1)$.*
3. *If $g \geq 2$, then P is diffeomorphic to $\Sigma_g \times S^2$*

Proof. For the genus one case see [BK, Lemma 10]. The other cases are well known. □

3. Simple wrinkled fibrations over general base surfaces

We are finally ready to introduce the main objects of study in this paper.

Definition 3.1. Let X be a 4-manifold and B a surface, both oriented. A *simple wrinkled fibration* with *total space* X and *base* B is a surjective smooth map of pairs $w\colon (X, \partial X) \to (B, \partial B)$ with the following properties:

1. w is a wrinkled fibration, i.e. $\mathcal{C}_w$ contains only indefinite folds and cusps,
2. $\mathcal{C}_w \cap \partial X = \emptyset$,
3. $\mathcal{C}_w$ is non-empty, connected, and contains a cusp,
4. w is injective on $\mathcal{C}_w$ and
5. all fibers of w are connected.

Two simple wrinkled fibrations $w\colon X \to B$ and $w'\colon X' \to B'$ are *equivalent* if there are orientation preserving diffeomorphisms $\hat{\phi}\colon X \to X'$ and $\check{\phi}\colon B \to B'$ such that $w' \circ \hat{\phi} = \check{\phi} \circ w$.

Since we assume the base and total space of a simple wrinkled fibration to be oriented, the regular fibers are closed, oriented surfaces (of varying genus as explained below). We can thus define the *genus* of w as the maximal genus among all regular fibers. A neighborhood of the critical image of a simple wrinkled fibration is shown in Figure 4

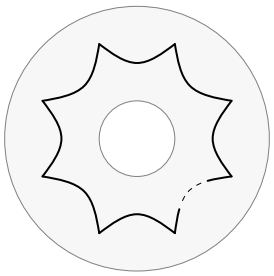

Figure 4. A neighborhood of the critical image of a simple wrinkled fibration.

Before we continue we make some remarks about the definition.

Remark 3.2. Simple wrinkled fibrations over S^2 are essentially the same as Williams' simplified purely wrinkled fibrations with two minor differences. One one hand we do not put restrictions on the fiber genus but on the other we require the presence of cusps. Both conditions can always be achieved by applying a *flip-and-slip move* (see Remark 3.3 below) and are thus merely of technical nature. Moreover, the "simple wrinkled fibrations without cusps" are easily classified (see Example 3.8) so that one does not lose too much by ignoring them.

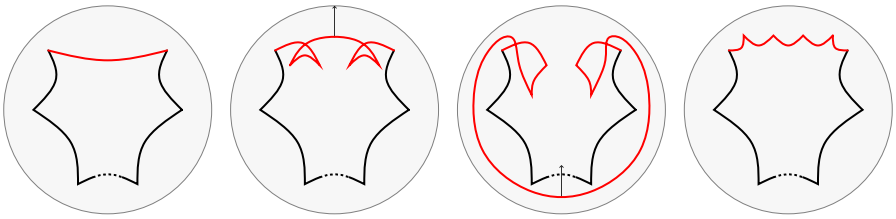

FIGURE 5. The base diagrams during a flip-and-slip move. (The pictures show the complement of a disk in the lower genus region of the original fibration.)

Remark 3.3. Given a simple wrinkled fibration over S^2 there is an important homotopy to another such simple wrinkled fibration which has become known as a *flip-and-slip move*. Its effect on the base diagram is shown in Figure 5. One first perform two flips on the same fold arc and then chooses an isotopy of the total space (the *slip*) during which the critical image undergoes the changes demonstrated in the picture. A flip-and-slip increases the fiber genus by one and introduces four new cusps.

Remark 3.4. In spite of the lengthy definition, simple wrinkled fibrations are arguably the simplest possible maps from 4-manifolds to surfaces, at least as far as their singularity structure is concerned. As will be explained in detail it is this simplicity which makes it possible to give nice combinatorial descriptions of 4-manifolds.

Remark 3.5. So far simple wrinkled fibrations have usually been studied up to homotopy instead of equivalence. However, we believe that the former point of view does not interact well with surface diagrams (which will be introduced momentarily) while the latter fits in perfectly. It would be interesting to relate the concepts of homotopy and equivalence but to our knowledge there is no obvious way to do so.

Given the rather specialized nature of simple wrinkled fibrations one might wonder whether they actually exist. This is indeed the case and we begin by giving some simple constructions.

Example 3.6 (Surface bundles)**.** Let $\pi\colon X \to B$ be a surface bundle over a surface B with closed fibers of genus g. Then we can perform a birth homotopy on π to obtain a genus $g+1$ simple wrinkled fibration with two cusps.

Example 3.7 (Lefschetz fibrations)**.** If $f\colon X \to B$ is a Lefschetz fibration (possibly achiral) with closed fibers of genus g, then after wrinkling all the Lefschetz singularities we obtain a number of disjoint circles with three cusps in the critical image. By suitably merging cusps we can turn this configuration into a single circle resulting in a simple wrinkled fibration of genus $g+1$.

Example 3.8 (The case without cusps)**.** This example includes the broken Lefschetz fibration on S^4 from [ADK] that was mentioned in the introduction. Let Ω be a cobordism from Σ_g to Σ_{g-1} together with a Morse function $\mu\colon \Omega \to I$ with exactly one critical point of index two. Then $\mu \times \mathrm{id}\colon \Omega \times S^1 \to I \times S^1$ is a stable map with one circle of indefinite folds which fails to be a simple wrinkled fibration only because it does not have any cusps. Nevertheless, we can use $\Omega \times S^1$ to build wrinkled fibrations over S^2 by suitably filling in the two boundary components with $\Sigma_g \times D^2$ and $\Sigma_{g-1} \times D^2$ such that the fibration structures on the boundary extends. Using the handle decomposition constructed in [B2] it is easy to see that this constructions one gives the following total spaces: $P\#S^1 \times S^3$ where P is any

Σ_{g-1}-bundle over S^2 and, if $g = 1$, S^4 and some other manifolds with finite cyclic fundamental group (see [BK, H1]). Having build these maps one can then apply a flip-and-slip to obtain honest simple wrinkled fibrations. In particular, we see that S^4 carries a simple wrinkled fibration of genus two.

As a side remark, the above mentioned genus one fibration on S^4 already appeared in [ADK] and is probably the reason why people became interested in constructing broken fibrations on general 4-manifolds.

The above examples show that simple wrinkled fibrations can be considered as a common generalization of surface bundles and (achiral) Lefschetz fibrations. The vastness of this generalization is indicated by the following remarkable theorem.

Theorem 3.9 (Williams [W1])**.** *Let X be a closed, oriented 4-manifold. Then any map $X \to S^2$ is homotopic to a simple wrinkled fibration of arbitrarily high genus.*

Remark 3.10. Williams' proof builds on results of Gay and Kirby [GK1] which, in turn, depend on deep theorems in 3-dimensional contact topology[4]. This somewhat unnatural dependence could be removed by refining the singularity theory based approach of [B1] to produce maps which are injective on their critical points.

Williams [W1] also introduced a combinatorial description of simple wrinkled fibrations over S^2 in terms of what he calls *surface diagrams*. In the remainder of this section we will generalize his construction to the setting of general base surfaces and prove a precise correspondence. Along the way we will see how simple wrinkled fibrations give rise to handle decompositions. In Section 4 we will return to Williams' surface diagrams and use them to prove some results.

Let $w\colon X \to B$ be a simple wrinkled fibration. As explained in Section 2.1, it follows from the definition of simple wrinkled fibrations that the critical locus $\mathcal{C}_w \subset X$ of a simple wrinkled fibration $w\colon X \to B$ is a smoothly embedded circle and that w restricts to a topological embedding of $\mathcal{C}_w$ into B. Furthermore, the critical image $w(\mathcal{C}_w)$ separates B into two components. Indeed, if its complement were connected, then all regular fibers would be diffeomorphic. But according to the fold model, the topology of the fibers on the two sides of a fold arc must be different. In fact, since we require that all fibers are connected, the genus on one side has to be one higher than on the other side. We will call the two components of $B \setminus w(\mathcal{C}_w)$ the *higher* (resp. *lower*) *genus region*.

We would like to understand more precisely how the topology of the fibers changes across the critical image. A *reference path* for w is an oriented, embedded arc $R \subset B$ that connects a point p_+ in the higher genus region to a point p_- in the lower genus region and intersects $w(\mathcal{C}_w)$ transversely in exactly one fold point. Then the *reference fibers* $\Sigma_\pm(R) := w^{-1}(p_\pm)$ over the *reference points* $p_\pm$ are closed, oriented surfaces.

Lemma 3.11. *A reference path $R \subset B$ induces a nonseparating simple closed curve $\gamma(R) \subset \Sigma_+(R)$ which depends only on the isotopy class of R relative to its reference points and the cusps.*

Definition 3.12. The curve $\gamma(R) \subset \Sigma_+(R)$ is called the *(fold) vanishing cycle* associated to R.

Proof. The fold model implies that $w^{-1}(R)$ is a cobordism from $\Sigma_+(R)$ to $\Sigma_-(R)$ on which w restricts to a Morse function with exactly one critical point of index 2. Thus $w^{-1}(R)$ is diffeomorphic to $\Sigma_+(R) \times [0, 1]$ with a (3-dimensional) 2-handle

[4]Eliashberg's classification of overtwisted contact structures and the Giroux correspondence between contact structures and open book decompositions

attached along a simple closed curve in $\Sigma_+(R) \times \{1\}$ which is canonically identified with a simple closed curve $\gamma(R) \subset \Sigma_+(R)$. □

Next, let us look at what happens around the cusp. Let R_1 and R_2 be two reference paths for w with common reference points and assume that their interiors are disjoint. We call R_1 and R_2 *adjacent* if their union $R_1 \cup R_2$ bounds a disk in B that contains exactly one cusp.

Lemma 3.13. *Let R_1 and R_2 be adjacent reference paths. Then the vanishing cycles $\gamma(R_1)$ and $\gamma(R_2)$ in $\Sigma_+ := \Sigma_+(R_1) = \Sigma_+(R_2)$ are geometrically dual.*

Proof. As in the proof of Lemma 3.11 the preimages $w^{-1}(R_i)$, $i = 1, 2$, are both cobordisms from Σ_+ to Σ_-, each consisting of a 2-handle attachment along $\gamma(R_i)$. By reversing the orientation of R_1 we can consider $w^{-1}(R_1)$ as a cobordism from Σ_- to Σ_+, now consisting of a 1-handle attachment. In this process the former attaching sphere of the 2-handle $\gamma(R_1)$ becomes the belt sphere of the 1-handle.

Gluing $w^{-1}(R_1)$ and $w^{-1}(R_2)$ together along Σ_+ gives a cobordism from Σ_- to itself consisting of a 1-handle attachment followed by a 2-handle attachment. Now recall that the cusp singularity models the death (or birth) of a canceling pair of critical points. Hence, the attaching sphere of the 2-handle, which is $\gamma(R_2)$, intersects the belt sphere of the 1-handle, which is $\gamma(R_1)$, in a single point. □

Looking a bit ahead, our strategy will be to choose suitable collections of reference paths and to study simple wrinkled fibrations in terms of the induced collection of vanishing cycles. The only obstacle for doing so is the possibly complicated topology of the base surface. But this can easily be overcome by the following observation. We can cut the base into three pieces

$$B = B_+ \cup A \cup B_-$$

where A is a regular neighborhood of the critical image of w (diffeomorphic to an annulus) and $B_\pm$ are the closures of the complement of A. The subscript in $B_\pm$ indicates whether the surface is contained in the higher or lower genus region. Note that w restricts to surface bundles over $B_\pm$ and, although complicated, these are a rather well studied class of objects. Thus the interesting new part of w is the restriction $w^{-1}(A) \to A$ which is a simple wrinkled fibration over an annulus. Moreover, this fibration has the property that the critical image does not bound a disk in A or, in other words, it is boundary parallel.

Definition 3.14. A simple wrinkled fibration $w\colon W \to A$ over an annulus A is called *annular* if its critical image is boundary parallel.

So in order to understand simple wrinkled fibrations over any base surface, it is enough to understand annular simple wrinkled fibrations and this is where surface diagrams enter the picture. The remainder of this section is devoted to proving the following theorem.

Theorem 3.15. *There is a bijective correspondence between annular simple wrinkled fibrations up to equivalence and twisted surface diagrams up to equivalence*

We will split the proof of the theorem into the two obvious parts. The first part is the subject of Section 3.1 (see Proposition 3.26) and the second is treated in Section 3.3 (see Proposition 3.32). Along the way, we will see in Section 3.2 that, just as Lefschetz fibrations, annular simple wrinkled fibrations are directly accessible via handlebody theory.

Remark 3.16. Recently Gay and Kirby have published a result that contains Theorem 3.15 as a special case [GK4]. Although their methods are somewhat similar to ours we feel that our approach is of independent interest.

3.1. **Twisted surface diagrams of annular simple wrinkled fibrations.** Consider an annular simple wrinkled fibration $w\colon W \to A$. We denote by $\partial_\pm A$ the boundary components of the base annulus A contained in the higher (resp. lower) genus region and we let $\partial_\pm W = w^{-1}(\partial_\pm A)$.

Definition 3.17. Let $w\colon W \to A$ be an annular simple wrinkled fibration. A *reference system* $\mathcal{R} = \{R_1, \dots, R_c\}$ for w (where c is the number of cusps) is a collection of reference paths for w such that

(1) all reference paths have the same reference points $p_\pm \in \partial_\pm A$,
(2) the interiors of the arcs are pairwise disjoint,
(3) with respect to the orientations on $\partial_\pm A$ the arcs leave $\partial_+ A$ and enter $\partial_- A$ in order of increasing index (see Figure 6) and
(4) each fold arc is hit by exactly one of the R_i.

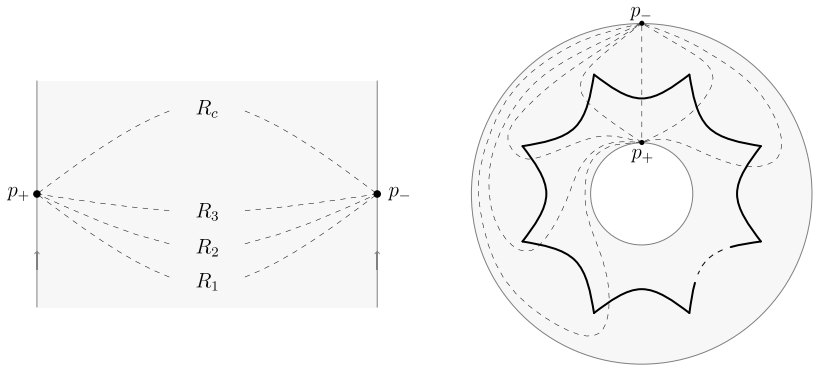

FIGURE 6. A reference system for an annular simple wrinkled fibration.

As before, we denote the reference fibers by $\Sigma_\pm := \Sigma_\pm(\mathcal{R}) = w^{-1}(p_\pm)$. Using the reference fibers we can write $\partial_\pm W$ as mapping tori

$$\partial_\pm W \cong \Sigma_\pm(\mu_\pm)$$

where $\mu_\pm \in \mathcal{M}(\Sigma_\pm)$ is the monodromy of w over $\partial_\pm A$ (in the positive direction). We will refer to μ_+ (resp. μ_-) as the *higher* (resp. *lower*) *monodromy* of w.

Lemma 3.18. *Let $w\colon W \to A$ be an annular simple wrinkled fibration together with a reference system $\mathcal{R} = \{R_1, \dots, R_c\}$ and let $\gamma_i = \gamma(R_i) \subset \Sigma_+$. Then for $i < c$ the vanishing cycles γ_i and γ_{i+1} are geometrically dual and, moreover, so are $\mu_+(\gamma_c)$ and γ_1.*

In the proof of this Lemma and subsequent consideration we will need the following notion. Let B be an oriented surface and let $R \subset B$ be a proper arc which hits a boundary component $\partial_i B \subset \partial B$ transversely in a single point. We parametrize a small collar of $\partial_i B$ by $S^1 \times [0,1]$ in such a way that $\partial_i B$ corresponds to $S^1 \times \{1\}$, R corresponds to $\{1\} \times [0,1]$ and the induced orientations on $\partial_i B$ agree. We say that the arc R' which corresponds to

$$\left\{(e^{2\pi t}, t) \middle| t \in [0,1]\right\}$$

via the parametrization is obtained from R by *swinging once around* $\partial_i B$.

Remark 3.19. At first glance, swinging about a boundary component seems to be the same as applying a boundary parallel Dehn twist and up to isotopy this is indeed the case. However, there is a subtle difference since a boundary parallel Dehn twists is usually assumed to be supported in the interior of the surface and

thus fixes a small collar of the boundary point wise while the support of the swinging diffeomorphism goes right up to the boundary. This difference becomes important in the following situation.

Let S be another arc with the same properties as R such that R and S are disjoint in the interior of B and assume that S leaves $\partial_i B$ after R. If we swing S once around $\partial_i B$, then the resulting arc remains disjoint from R but now leaves $\partial_i B$ before R. On the other hand, if we perform a boundary parallel Dehn twist on S, then we keep the exit order at the price of introducing an interior intersection point. In particular, if $\mathcal{R} = \{R_1, \dots, R_c\}$ is a reference system for an annular simple wrinkled fibration, then we obtain a new reference system by swinging the last arc R_c once around each boundary component fo the annulus.

Proof of Lemma 3.18. The first statement follows from Lemma 3.13 since for $i < c$ the reference paths R_i and R_{i+1} are clearly adjacent. The second statement needs an additional arguments. We first swing R_c once around the boundary of A so that the resulting reference path R'_c is adjacent to R_1 and thus $\gamma(R'_c)$ is geometrically dual to $\gamma(R_1)$. Next we observe that R'_c is homotopic to R_c precomposed with the boundary curve. Thus the parallel transport along R'_c is the composition of the parallel transport along R_c and the higher genus monodromy. In particular, we have $\gamma(R'_c) = \mu_+(\gamma_c)$. □

Remark 3.20. Note that in the above proof we did not actually need the whole reference system but only the parts of the arcs contained in the higher genus region.

Let us isolate the combinatorial structures encountered in the above Lemma.

Definition 3.21. Let Σ be a surface. A *circuit* (of *length* c) on Σ is an ordered collection of simple closed curves $\Gamma = (\gamma_1, \dots, \gamma_c)$ such that any two adjacent curves γ_i and γ_{i+1} are geometrically dual for $i < c$. A *switch* for Γ is a mapping class $\mu \in \mathcal{M}(\Sigma)$ such that $\mu(\gamma_c)$ and γ_1 are geometrically dual. We say that Γ is *closed* if γ_c and γ_1 are geometrically dual, i.e. if the identity works as a switch.

Definition 3.22. A *twisted surface diagram* is a triple $\mathfrak{S} = (\Sigma, \Gamma, \mu)$ where Σ is a closed, oriented surface, Γ is a circuit in Σ and $\mu \in \mathcal{M}(\Sigma)$ is a switch for Γ.

Remark 3.23. There is no restriction on the intersections of non-adjacent curves in a circuit. Circuits in which non-adjacent curves are disjoint, so called *chains of curves*, are well known objects in the theory of mapping class groups of surfaces where they play an important role.

Remark 3.24. Sometimes it will be convenient to choose orientations on the curves in a circuit $\Gamma = (\gamma_1, \dots, \gamma_c)$ in order to speak of their homology classes. If the ambient surface is oriented, we will always choose orientations such that the intersection of γ_i and γ_{i+1}, $i < c$, has positive sign.

With this terminology we can rephrase Lemma 3.18 as stating that an annular simple wrinkled fibration $w\colon W \to A$ together with a reference system $\mathcal{R}$ induces a twisted surface diagram

$$\mathfrak{S}_{w,\mathcal{R}} := (\Sigma_+, \Gamma_{w,\mathcal{R}}, \mu_+)$$

where the higher monodromy works as a switch.

Note that when the higher monodromy is trivial we obtain a closed circuit and recover Williams' surface diagrams for which we shall reserve this name, i.e. in the following the term surface diagram will always mean a triple $(\Sigma, \Gamma, \mathrm{id})$ which we simply denote by (Σ, Γ) or sometimes even $(\Sigma; \gamma_1, \dots, \gamma_c)$. Whenever we allow nontrivial higher monodromy we will explicitly speak of twisted surface diagrams.

Not surprisingly, the twisted surface diagrams constructed in Lemma 3.18 depend on the choice of the reference system. To understand this dependence we

observe that a reference system is uniquely determined (up to isotopy relative to the boundary and the cusps) by specifying the first reference path – this follows directly from the definition. Furthermore, it is easy to see that any two reference paths which have the same reference points and hit the same fold arc become isotopic after suitably swinging around the boundary components of A.

Now let $\mathcal{R} = \{R_1, \dots, R_c\}$ and $\mathcal{S} = \{S_1, \dots, S_c\}$ be two reference systems with common reference points and let S_k hit the same fold arc as R_1. As in the proof of Lemma 3.18 we successively swing the arcs $S_c, S_{c-1}, \dots, S_k$ once around each boundary component to obtain a new reference system $\mathcal{S}'$ in which the first reference path hits the same fold arc as R_1. Now, by further swinging all of $\mathcal{S}'$ simultaneously, but this time independently around the boundary components, we can match the two first reference paths and thus the whole reference systems.

Let us analyze the effect of this matching procedure on the twisted surface diagram. For brevity of notation let $\mathfrak{S} = (\Sigma, \Gamma, \mu)$ be the twisted surface diagram associated to an annular simple wrinkled fibration $w\colon W \to A$ together with a reference system $\mathcal{R}$. Since the surface Σ and the switch μ only depend on the reference points, only the circuit $\Gamma = (\gamma_1, \dots, \gamma_c)$ will be affected by swinging some reference paths. Moreover, note again that the vanishing cycles γ_i only depend on the part of the reference paths contained in the higher genus region. Thus swinging around the lower genus boundary does not change the circuit.

Now, as we have already observed, if we swing the last reference path in $\mathcal{R}$ once around both boundary components, we obtain a new reference system $\mathcal{R}'$ and which induces the circuit

$$\Gamma_\mu^{[1]} := \big(\mu(\gamma_c), \gamma_1, \dots, \gamma_{c-1}\big).$$

This operation of going from $\mathfrak{S}$ to $\mathfrak{S}^{[1]} := (\Sigma, \Gamma_\mu^{[1]}, \mu)$ makes sense in the abstract setting of twisted surface diagrams and we call it (and its obvious inverse) *switching*. Note that if the higher monodromy μ is trivial, then switching amounts to a cyclic permutation of the vanishing cycles.

Since we can relate any two reference systems for a given annular simple wrinkled fibration by suitably swinging reference paths, we see that the twisted surface diagram is well defined up to switching.

Next we want to compare the twisted surface diagrams of two equivalent annular simple wrinkled fibrations as in the commutative diagram below.

$$\begin{array}{ccc} X & \xrightarrow{\hat{\phi}} & X' \\ {\scriptstyle w}\downarrow & & \downarrow{\scriptstyle w'} \\ A & \xrightarrow{\check{\phi}} & A' \end{array}$$

If $\mathcal{R}$ is a reference system for w, then $\mathcal{R}' := \check{\phi}(\mathcal{R})$ is a reference system for w'. Let $\mathfrak{S} = (\Sigma, \Gamma, \mu)$ and $\mathfrak{S}' = (\Sigma', \Gamma', \mu')$ be the associated twisted surface diagrams. Then $\hat{\phi}$ induces an orientation preserving diffeomorphism $\phi\colon \Sigma \to \Sigma'$ and clearly the higher monodromies satisfy $\mu' = \phi\mu\phi^{-1}$. It is also easy to see that

$$\Gamma' = \phi(\Gamma) := \big(\phi(\gamma_1), \dots, \phi(\gamma_c)\big)$$

where, as usual, $\Gamma = (\gamma_1, \dots, \gamma_c)$. Again, the effect of an equivalence of annular simple wrinkled fibrations makes sense for abstract twisted surface diagrams and we say that $\mathfrak{S}$ and $\mathfrak{S}'$ are *diffeomorhpic* via ϕ. Putting this together with switching we end up with the following definition.

Definition 3.25. Two twisted surface diagrams $\mathfrak{S}$ and $\mathfrak{S}'$ called *equivalent* if, for some integer k, $\mathfrak{S}'$ is diffeomorphic to $\mathfrak{S}^{[k]}$.

Summing up the content of this section we have proved the first half of Theorem 3.15:

Proposition 3.26. *To an annular simple wrinkled fibration $w\colon W \to A$ we can assign a twisted surface diagram*

$$\mathfrak{S}_w = (\Sigma_+, \Gamma_w, \mu_+)$$

which is well defined up to switching. Moreover, equivalent annular simple wrinkled fibrations have equivalent twisted surface diagram.

Remark 3.27. We would like to point out that it is very convenient that only the equivalence class of the surface diagram plays a role. Indeed, in order to actually visualize the twisted surface diagram of an annular simple wrinkled fibration one has to identify the higher genus reference fiber with some model surface and there is no canonical way to do so. However, any two such identifications will differ by a diffeomorphism of the model surface and thus be equivalent. So we can safely forget about the choice of identification whenever we are only interested in the equivalence class of the simple wrinkled fibrations or the diffeomorphism type of its total space.

3.2. **Handle decompositions for annular simple wrinkled fibrations.** As a next step we relate the twisted surface diagrams associated to annular simple wrinkled fibrations to the topology of their total spaces. We will see that the situation is very similar to Lefschetz fibrations

Proposition 3.28. *Let $w\colon W \to A$ be an annular simple wrinkled fibration. Then W has a relative handle decomposition on $\partial_+ W$ with one 2-handle for each fold arc. Such a handle decomposition is encoded in any twisted surface diagram for w.*

In the following we will refer to the 2-handles associated to the fold arcs as *fold handles*.

Proof. The rough idea is to parametrize A by the model annulus $S^1 \times [0,1]$ such that the composition of w and the projection $p\colon S^1 \times [0,1] \to [0,1]$ becomes a Morse function. The details go as follows.

We equip $S^1 \times [0,1]$ with coordinates (θ, t) refer to the direction in which t increases as *right*. We say that a parametrization $\kappa\colon A \to S^1 \times [0,1]$ is *w-regular* if the critical image $C_\kappa := \kappa \circ w(\mathcal{C}_w)$ is in the following *standard position*:

- all cusps point to the right
- each $R_\theta := \{\theta\} \times [0,1]$ meets C_κ in exactly one point, either in a cusp or transversely in a fold point and
- the projection p restricted to C_κ has exactly one minimum on each fold arc.

We claim that for any w-regular parametrization κ, the map

$$p_\kappa := p \circ \kappa \circ w\colon W \to [0,1]$$

is a Morse function. Clearly, the critical points of p_κ are contained in $\mathcal{C}_w$. Thus we have to understand how the projection p interacts with the critical image C_κ. By the standard position assumption there are three ways how a level set $S_t := S^1 \times \{t\}$ can intersect C_κ (see Figure 7):

a) S_t intersects C_κ transversely in a fold point,
b) S_t meets C_κ in a cusp and the fold arcs surrounding the cusp are on the left side of S_t or
c) S_t is tangent to a fold arc which is located on the right side of S_t. We will refer to this phenomenon as a *concave tangency*.

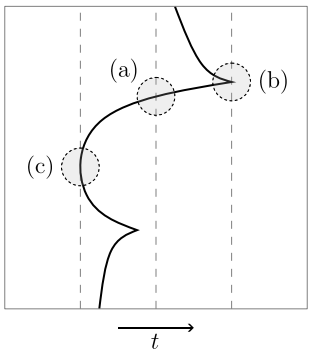

FIGURE 7. Level sets intersecting the critical image.

It turns out that only the concave tangencies contribute critical points of p_κ. In fact, from the models for the fold an cusp we immediately see that p_κ is modeled on the compositions

$$(t, x, y, z) \mapsto (t, -x^3 + 3tx - y^2 + z^2) \mapsto t \tag{3.1}$$

in case of a cusp intersection and

$$(t, x, y, z) \mapsto (t, -x^2 - y^2 + z^2) \mapsto \pm t \tag{3.2}$$

for a transverse fold intersection[5] which shows that these are regular points of p_κ.

It remains to treat the concave tangencies. These occur precisely at the minima of $p_\kappa|_{C_\kappa}$. This minimum can be modeled by $t \mapsto t^2$ and it is easy to see that p_κ is modeled on

$$(t, x, y, z) \mapsto (-x^2 - y^2 + z^2 + t^2) \tag{3.3}$$

which is a Morse singularity of index 2. By assumption there is exactly one concave tangency for each fold arc and, using the correspondence between Morse functions and handle decompositions, we obtain the desired handle decomposition.

In order to understand how the fold handles are attached consider the arcs $R_i := R_{\theta_i} \subset S^1 \times [0, 1]$ where $\theta_1, \dots, \theta_c \in S^1$ is a sequence of numbers ordered according to the orientation of S^1 (e.g. the c-th roots of unity). The w-regular parametrization κ can be chosen in such a way that each R_i is a reference path for precisely one fold arc and C_κ is contained in the open annulus $S^1 \times (\epsilon, 1 - \epsilon)$ for some $\epsilon > 0$. For each R_i we obtain a vanishing cycle γ_i in the fiber of w over $(\theta_i, 0) \in \partial_+ A$ and the local model for the fold singularity implies that the fold handles are attached to $\partial_+ W \times [0, \epsilon]$ along the vanishing cycles γ_i pushed off into the fiber over (θ_i, ϵ) with respect to the canonical framing induced by the fiber.

The relation to twisted surface diagrams now becomes obvious. There is a canonical way to turn the reference paths $\Theta_1, \dots, \Theta_c$ into a reference system by fixing Θ_1 and successively sliding the endpoints of the remaining arcs along the boundary onto Θ_1 against the orientation. Thus the vanishing cycles record the attaching curves of the fold handles. □

Remark 3.29. The above proposition is one of the reasons that made us require the presence of cusps in the critical loci of simple wrinkled fibrations. If there were no cusps, then it would not be possible to avoid *convex tangencies* which correspond to 3-handles instead of 2-handles. Thus the presence of cusps guarantees that the total spaces of annular simple wrinkled fibrations are (relative) 2-handlebodies.

[5]The sign depends on how the fold and cusp models are embedded.

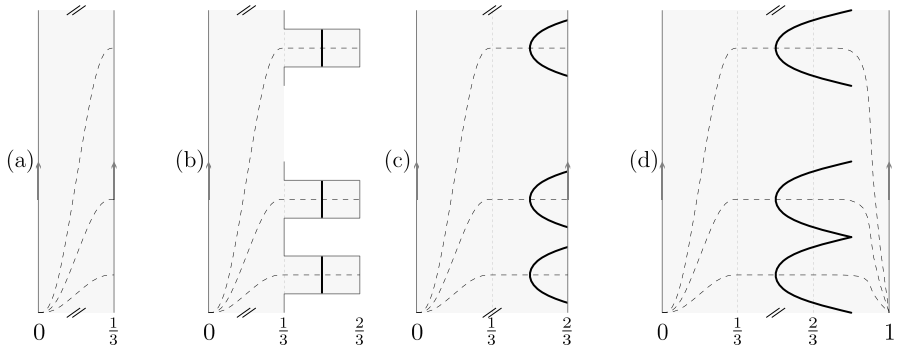

FIGURE 8. Building a simple wrinkled fibration from a surface diagram. (bold: critical image, dashed: reference path)

Remark 3.30. The observation that fold tangencies correspond to Morse singularities also appears in [GK2] in their more general setting of Morse 2-functions. The fact that the real part of the Lefschetz model is also a Morse function allows to include Lefschetz singularities in the discussion. Proceeding this way, one can recover Baykur's result about handle decompositions from broken Lefschetz fibrations (see [B2]).

Remark 3.31. The reader familiar with Lefschetz fibrations will have noticed the strong resemblance of the handle decompositions described above with the ones induces by Lefschetz fibrations. In fact, the handle decompositions have exactly the same structure except that the fold handles are attached with respect to the fiber framing while the framing of the *Lefschetz handles* differs by -1.

3.3. **Annular simple wrinkled fibrations from twisted surface diagrams.** Using the handle decompositions exhibited in the previous section as a stepping stone we can now build annular simple wrinkled fibrations out of twisted surface diagrams and thus complete the proof of Theorem 3.15.

Proposition 3.32. *A twisted surface diagram $\mathfrak{S} = (\Sigma, \Gamma, \mu)$ determines an annular simple wrinkled fibration $w_{\mathfrak{S}} \colon W_{\mathfrak{S}} \to S^1 \times [0,1]$ with higher genus fiber Σ and higher monodromy μ.*

Proof. To make the construction of $w_{\mathfrak{S}}$ more transparent we begin with some preliminary considerations.

One important ingredient is the mapping cylinder $\Sigma(\mu)$ which is equipped with a canonical fibration $p \colon \Sigma(\mu) \to S^1$. Given the construction of $\Sigma(\mu)$ it is convenient to consider S^1 as the quotient $[0,1]/\{0,1\}$ and we will identify Σ with the fiber over the point $0 \sim 1$.

We will now describe a collection of arcs $\mathcal{R} = \{R_1, \dots, R_c\}$ in $S^1 \times [0,1]$, which we consider as

$$S^1 \times [0,1] = [0,1] \times [0,1]/(0,t) \sim (1,t),$$

that will serve as a reference system for $w_{\mathfrak{S}}$ (see Figure 8 (a)).

Let $r \colon [0,1] \to [0,1]$ be a smooth function that has the constant value 1 on the interval $[\frac{1}{3}, \frac{2}{3}]$, satisfies $r(0) = r(1) = 0$ and is strictly increasing (resp. decreasing) for $t \leq \frac{1}{3}$ (resp. $t \geq \frac{2}{3}$). If the length of Γ is c, then for $i = 1, \dots, c$ we let $\theta_i := \frac{i-1}{c}$ and define

$$R_i := \big\{ \big(\theta_i r(t), t\big)/\sim \;\big|\; t \in [0,1] \subset S^1 \times [0,1] \big\}$$

We these remarks in place we can now begin with the construction of $W_{\mathfrak{S}}$ and $w_{\mathfrak{S}}$. This will be done in three steps.

Step 1: We begin by taking the product

$$W_1 := \Sigma(\mu) \times [0, \tfrac{1}{3}]$$

and define a map $w_1 \colon W_1 \to S^1 \times [0, \frac{1}{3}]$ by sending (x, t) to $(p(x), t)$.

Step 2: Next, we construct W_2 by attaching 2-handles to W_1 in the following way. Let $\Gamma = (\gamma_1, \dots, \gamma_c)$. Using the arc $R_i \subset S^1 \times [0, 1]$ described above we can parallel transport the curve $\gamma_i \subset \Sigma$ to the fiber of w_1 over $(\theta_i, \frac{1}{3})$. We attach a 2-handle to the resulting curve with respect to the fiber framing.

This choice of framing allows us to extend w_1 over each 2-handle. Indeed, we can consider attaching the i-th (4-dimensional) 2-handle as a 1-parameter family of 3-dimensional 2-handle attachments parametrized by a small neighborhood of $(\theta_i, 1)$ in $S^1 \times \{1\}$. (Of course, these neighborhoods are pairwise disjoint.) For each point θ in such a neighborhood, the restriction of w_1 to the *θ-ray* $\{\theta\} \times [0, \frac{1}{3}]$ extends to a Morse function (with one critical point of index 2) over a slightly longer ray, say $\{\theta\} \times [0, \frac{2}{3}]$, in the standard way. Using these 1-parameter families of Morse functions we can extend w_1 to map from W_2 to an annulus with "bumps" on one side as shown in Figure 8 (b) and this map has an arc of indefinite folds on each bump. We can then smooth out the bumps by standard techniques from differential topology to obtain a map $w_2 \colon W_2 \to S^1 \times [0, \frac{2}{3}]$ in which each 2-handle attachment has created an arc of indefinite folds whose endpoints hit the boundary of W_2 transversely in the component that was affected by the handle attachment (Figure 8 (c)), let us call this component $\partial_2 W_2$

Step 3: For the final step we first note that the restriction of w_2 over $S^1 \times \{\frac{2}{3}\}$ is a circle valued Morse function with a pair of critical points of index 1 and 2 for each fold arc of w_2. The crucial observation is that the condition that Γ is a circuit with switch μ implies that all these pairs of critical points cancel! Thus there is a standard homotopy, which we parametrize by $[\frac{2}{3}, 1]$, from $w_2|_{\partial_2 W_2}$ to a submersion that realizes this cancellation. We let

$$W_{\mathfrak{S}} := W_2 \cup_{\partial_2 W_2} \partial_2 W_2 \times [\tfrac{2}{3}, 1]$$

and extend w_2 by tracing out the homotopy over the newly added collar of $\partial_2 W_2$ to obtain a map $w_{\mathfrak{S}} \colon W_{\mathfrak{S}} \to S^1 \times [0, 1]$. This last step removes all critical points from the boundary and introduces an interior cusp for any canceling pair. Clearly $w_{\mathfrak{S}}$ is an annular simple wrinkled fibration with base diagram as in Figure 8 (d).

Note that $W_{\mathfrak{S}}$ is diffeomorphic to W_2 and thus has the same relative handle decomposition. Moreover, it follows directly from the construction that $\mathcal{R}$ is a reference system for $w_{\mathfrak{S}}$ with $\mathfrak{S}$ as its twisted surface diagram. □

In order to finish the proof of Theorem 3.15 we have to show that equivalent twisted surface diagram give equivalent annular simple wrinkled fibrations. Recall that an equivalence of surface diagram is a combination of two things: switching and a diffeomorphism. We will treat these separately.

Lemma 3.33. *If $\mathfrak{S}$ and $\mathfrak{S}'$ are diffeomorphic, then $w_{\mathfrak{S}}$ and $w_{\mathfrak{S}'}$ are equivalent.*

Proof. Let $\mathfrak{S} = (\Sigma, \Gamma, \mu)$, $\mathfrak{S}' = (\Sigma', \Gamma', \mu')$ and let $\phi \colon \Sigma \to \Sigma'$ be a diffeomorphism such that $\Gamma' = \phi(\Gamma)$ and $\mu' = \phi\mu\phi^{-1}$. We will extend ϕ to a diffeomorphism $\hat{\phi} \colon W_{\mathfrak{S}} \to W_{\mathfrak{S}'}$ which fits in the commutative diagram

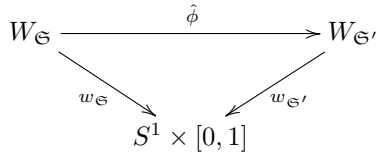

This will be done by going through the steps in the proof of Proposition 3.32. Let W_i and W_i', $i = 1, 2$, denote the 4-manifolds build in each step.

The condition $\mu' = \phi\mu\phi^{-1}$ shows that ϕ induces a fiber preserving diffeomorphism $\Sigma(\mu) \to \Sigma'(\mu')$. Taking the product with the identity, we obtain $\hat{\phi}_1 \colon W_1 \to W_1'$.

In the second step, where the 2-handles are attached to the curves in Γ, we simply note that $\hat{\phi}_1$ maps the attaching regions into each other and can thus be extended over the 2-handles to $\hat{\phi}_2 \colon W_2 \to W_2'$. Note that the smoothing of the bumpy annulus does not cause any trouble since it does not involve the total space.

For the third step observe that, given a homotopy from $w_2|_{\partial_2 W_2}$ to a submersion, we can push it forward via $\hat{\phi}_2|_{\partial_2 W_2}$ to obtain such a homotopy for $w_2'|_{\partial_2 W_2'}$. □

Lemma 3.34. *If $\mathfrak{S}$ is a twisted surface diagram, then $w_{\mathfrak{S}}$ and $w_{\mathfrak{S}^{[1]}}$ are equivalent.*

Proof. If we take the canonical reference system for $w_{\mathfrak{S}}$ and swing the last reference path once around the boundary, we obtain a reference system which induces $\mathfrak{S}^{[1]}$. Thus $w_{\mathfrak{S}}$ and $w_{\mathfrak{S}^{[1]}}$ can be considered as the same annular simple wrinkled fibration. □

Combining these two lemmas we obtain

Corollary 3.35. *If $\mathfrak{S}$ and $\mathfrak{S}'$ are equivalent, then so are $w_{\mathfrak{S}}$ and $w_{\mathfrak{S}'}$.*

3.4. **Gluing ambiguities.** Now that we know how to study annular simple wrinkled fibrations in terms of their twisted surface diagrams, recall that simple wrinkled fibrations over arbitrary base surfaces can be obtained from an annular ones by gluing suitable surface bundles to the boundary components. To be precise, let $w_0 \colon W \to A$ be an annular simple wrinkled fibration and let $\pi_\pm \colon Y_\pm \to B_\pm$ be surface bundles over surfaces $B_\pm$ such that there are boundary components $C_\pm \subset B_\pm$ and fiber preserving diffeomorphisms $\psi_\pm \colon \pi_\pm^{-1}(C_\pm) \to \partial_\pm W$. Then we can form a simple wrinkled fibration

$$w \colon Y_+ \cup_{\psi_+} W \cup_{\psi_-} Y_- \longrightarrow B_+ \cup_{C_+} A \cup_{C_-} B_-.$$

Of course, different choices of gluing diffeomorphisms may lead to inequivalent simple wrinkled fibrations. If we fix a pair $\psi_\pm$ of gluing maps, then we can obtain any other such pair by composing with automorphisms (in the sense of Section 2.2.2) of the boundary fibrations $w_0 \colon \partial_\pm W \to S^1$. Obviously, isotopic gluing maps give rise to equivalent simple wrinkled fibrations and the gluing ambiguities are a priori parametrized by

$$\pi_0\big(\operatorname{Aut}(\partial_+ W, w)\big) \times \pi_0\big(\operatorname{Aut}(\partial_- W, w)\big)$$

However, it turns out that the first factor can be eliminated.

Lemma 3.36. *Let $w \colon W \to A$ be an annular simple wrinkled fibration. Then any fiber preserving diffeomorphism of $\partial_+ W$ extends to an auto-equivalence of w.*

Proof. By Theorem 3.15 we can assume that w is built from a twisted surface diagram $\mathfrak{S} = (\Sigma, \Gamma, \mu)$ such that $\partial_+ W = \Sigma(\mu)$. According to (2.6) there are two types of automorphisms of $\Sigma(\mu)$, the *constant* ones coming from $C_{\mathcal{M}(\Sigma)}(\mu)$ and the *non-constant* ones originating from $\pi_1(\operatorname{Diff}(\Sigma), \mathrm{id})$. The statement that constant automorphisms of $\partial_+ W$ extend to auto-equivalences of w is just a reformulation of Lemma 3.33. Thus it remains to treat the non-constant ones.

Recall that by Theorem 2.9 these only occur when Σ has genus one. We can thus assume that $\Sigma = T^2$. A well known refinement of Theorem 2.9 states that the map

$$\pi_1\big(\operatorname{Diff}(T^2), \mathrm{id}\big) \to \pi_1(T^2, x) \tag{3.4}$$

which sends an isotopy to the path traced out by a base point $x \in T^2$ during that isotopy is an isomorphism (see [EE]). Note that the fundamental group of T^2 is

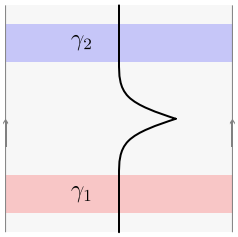

FIGURE 9. The relevant regions for extending non-constant automorphisms.

generated by the curves γ_1 and γ_2 (after choosing orientations, of course) if we take their unique intersection point as base point. Hence, we only have to extend the automorphisms coming from generators of $\pi_1\big(\mathrm{Diff}(T^2), \mathrm{id}\big)$ mapping to γ_1 and γ_2 in (3.4). If one parametrizes the torus by $S^1 \times S^1 \subset \mathbb{C}^2$ such that $S^1 \times \{1\}$ maps to γ_1 and $\{1\} \times S^1$ maps to γ_2, then such generators are given by

$$h_t^{\gamma_1}(\xi, \eta) := \big(e^{2\pi i\, t}\xi, \eta\big) \quad \text{and} \quad h_t^{\gamma_2}(\xi, \eta) := \big(\xi, e^{2\pi i\, t}\eta\big) \qquad (t \in [0, 1])$$

and we denote the corresponding automorphisms of $\Sigma(\mu)$ by

$$\varphi_i(x, t) := \big(h_t^{\gamma_i}(x), t\big).$$

In order to extend φ_i to $Z_{\mathfrak{S}}$ we take one step back and homotope the path h^{γ_i} to be constant outside the interval where the 2-handle corresponding to γ_i is attached. These intervals (times [0,1]) are highlighted in Figure 9. Outside the preimage of the regions shown in Figure 9 we can simply extend φ_i as the identity. In these region, observe that $h_t^{\gamma_i}$ fixes γ_i set wise at all times, it just rotates it more and more as t increases. It is easy to see that these rotations can be extended across the 2-handles in a way that respects the fibration structure. □

Remark 3.37. The genus one case of Example 3.8 shows that this Lemma does not hold without in the absence of cusps. The above proof breaks down at the point where we need the vanishing cycles to generate the fundamental group.

4. Simple wrinkled fibrations over the disk and the sphere

We now leave the general theory behind and focus on untwisted surface diagrams, i.e. pairs (Σ, Γ) where Γ is a closed circuit in Σ. By the correspondence established in the previous section such a surface diagram corresponds to an annular simple wrinkled fibration whose higher genus boundary component has trivial monodromy. We can thus fill this boundary component with $\Sigma \times D^2$ using some fiber preserving diffeomorphism of $\Sigma \times S^1$ to obtain a simple wrinkled fibration over the disk. (Note that the boundary of the disk is contained in the lower genus region; we will refer to such fibrations as *descending* simple wrinkled fibrations over the disk.) Furthermore, by Lemma 3.36 different choices of gluing diffeomorphisms produce equivalent simple wrinkled fibrations. Altogether, we have established the following.

Proposition 4.1. *There is bijective correspondence between (untwisted) surface diagrams up to equivalence and descending simple wrinkled fibrations over the disk up to equivalence.*

As mentioned before, when we speak of surface diagrams, we will always mean untwisted surface diagrams. This will not lead to confusion since we will not encounter any twisted surface diagrams anymore.

For a surface diagram $\mathfrak{S} = (\Sigma, \Gamma)$ we denote the corresponding simple wrinkled fibration by $w_{\mathfrak{S}} \colon Z_{\mathfrak{S}} \to D^2$ or, by a slight abuse of notation, simply by $Z_{\mathfrak{S}}$ with the

map to the disk implicitly understood. The boundary of $Z_{\mathfrak{S}}$ fibers over S^1 and if this boundary fibration is trivial, then we can *close off* to a simple wrinkled fibration over S^2. Recall that Theorem 3.9 tells us that we can obtain *all* smooth, closed, oriented 4-manifolds by this process. It is thus of great interest to understand which surface diagrams describe closed 4-manifolds. The following example indicates that this might be a hard problem.

Example 4.2. Let Σ be a closed, orientable surface together with a mapping class $\phi \in \mathcal{M}(\Sigma)$. Then any factorization of μ into positive Dehn twists yields a Lefschetz fibration over the disk whose boundary can be identified with the mapping torus $\Sigma(\phi) = (\Sigma \times [0,1])/(x,1) \sim (\phi(x),0)$. As in Example 3.7 we can turn this Lefschetz fibration into a descending simple wrinkled fibration without changing the boundary. Thus any surface bundle over the circle (with closed fibers) bounds some descending simple wrinkled fibration over the disk and any mapping class can be realized as the monodromy of a surface diagram.

In fact, the situation is very similar to the theory of Lefschetz fibrations. Any word in positive Dehn twists (or, equivalently, a finite sequence of simple closed curves) on a closed, oriented surface determines a Lefschetz fibration over the disk, the boundary fibers over the circle with monodromy given by the product of the Dehn twists and if this monodromy is trivial, then one can close off to a Lefschetz fibration over S^2. Just as an arbitrary product of Dehn twists will will not be isotopic to the identity, a surface diagram will not give rise to a simple wrinkled fibration over S^2. The advantage of the Lefschetz setting is the direct control over the boundary.

4.1. **The monodromy of a surface diagram.** In order to obtain a more intrinsic description of the boundary of $Z_{\mathfrak{S}}$ in terms of $\mathfrak{S}$ we need a little detour.

Let $a, b \subset \Sigma$ be a pair of simple closed curves in a surface Σ that intersect transversely in a single point. We denote by Σ_a and Σ_b the surfaces obtained by surgery on the curves a and b, respectively. To be concrete, we fix tubular neighborhoods νa and νb and picture Σ_a (resp. Σ_b) as the result of filling in the two boundary components of $\Sigma \setminus \nu a$ (resp. $\Sigma \setminus \nu b$) with disks. By the assumption on intersections we can assume that $\nu(a \cup b) := \nu a \cup \nu b$ is diffeomorphic to a once punctured torus – for convenience we will also assume that it has a smooth boundary in Σ. Observe that $\Sigma \setminus \nu(a \cup b)$ has one boundary component and is contained in both Σ_a and Σ_b as a subsurface. Furthermore, the closure of $\nu b \setminus \nu a$ (resp. $\nu a \setminus \nu b$) is a disk in Σ_a (resp. Σ_b). It follows that, up to isotopy, there is a unique diffeomorphism

$$\kappa_{a,b} \colon \Sigma_a \to \Sigma_b$$

which can be assumed to map $\nu b \setminus \nu a$ onto $\nu a \setminus \nu b$.

Now let $\mathfrak{S} = (\Sigma; \gamma_1, \dots, \gamma_l)$ be a surface diagram and consider the associated simple wrinkled fibration $w_{\mathfrak{S}} \colon Z_{\mathfrak{S}} \to D^2$. Then each adjacent pair of curves γ_i and γ_{i+1} fits the above situation and we thus get a collection of diffeomorphisms

$$\kappa_{\gamma_i,\gamma_{i+1}} \colon \Sigma_{\gamma_i} \to \Sigma_{\gamma_{i+1}}.$$

Moreover, it follows from the definition of surface diagrams that the composition

$$\mu_{\mathfrak{S}} := \kappa_{\gamma_c,\gamma_1} \circ \kappa_{\gamma_{c-1},\gamma_c} \circ \dots \circ \kappa_{\gamma_1,\gamma_2}$$

maps Σ_{γ_1} to itself and it is easy to see that its isotopy class does not depend on any of the implicit choices involved in its definition.

Definition 4.3. The mapping class $\mu_{\mathfrak{S}} \in \mathcal{M}(\Sigma_{\gamma_1})$ represented by the diffeomorphism above is called the *monodromy* of $\mathfrak{S}$.

This name is justified by the following lemma.

Lemma 4.4. *Let $\mathfrak{S} = (\Sigma, \Gamma)$ be a surface diagram. Then the boundary fibration $(\partial Z_{\mathfrak{S}}, w_{\mathfrak{S}})$ can be identified with the mapping torus $\Sigma_{\gamma_1}(\mu_{\mathfrak{S}})$.*

Proof. By the construction of $w_{\mathfrak{S}}$ its fiber over the origin is naturally identified with Σ. Furthermore, recall that the annular fibration associated to $\mathfrak{S}$ is equipped with a reference system whose reference paths we can naturally extend from the annulus to the disk by connecting them to the origin. The result is a collection of reference paths $R_1, \dots, R_c$ from the origin to the boundary of the disk and we denote its endpoints by $\theta_1 \dots, \theta_c \in S^1$. Observe that such a reference path, R_i say, gives rise to an identification of the fiber over θ_i with the surface Σ_{γ_i} obtained from surgery on γ_i where γ_i is the vanishing cycle associated to R_i.

Now consider the region in the base bounded by two adjacent reference path R_i and R_{i+1}. Using a suitable notion of parallel transport we see that the preimage of this region contains a trivial bundle with fiber $\Sigma \setminus \nu(\gamma_i \cup \gamma_{i+1})$. In particular, the parallel transport along the boundary segment from θ_i to θ_{i+1} restricts to the identity on the complement of $\nu(\gamma_i \cup \gamma_{i+1})$ and thus must be isotopic to $\kappa_{\gamma_i, \gamma_{i+1}}$ and the claim follows. □

It is also possible to describe the monodromy in terms of the original surface Σ. This takes us on another small detour. Let $a \subset \Sigma$ be a non-separating simple closed curve in a surface Σ and let $\mathcal{M}(\Sigma, a)$ denote the subgroup of $\mathcal{M}(S)$ consisting of all elements that fix a up to isotopy. It is well known that there is a short exact sequence[6]

$$1 \longrightarrow \langle \tau_a \rangle \longrightarrow \mathcal{M}(\Sigma, a) \xrightarrow{\mathrm{cut}_a} \mathcal{M}(\Sigma \setminus a) \longrightarrow 1 \tag{4.1}$$

where $\Sigma \setminus a$ is viewed as a twice punctured surface. The complement $\Sigma \setminus a$ can be related to the surgered surface Σ_a as follows. In Σ_a there is an obvious pair of points, namely the centers of the surgery disks. If we denote by Σ_a^* the surface obtained by marking these points, then $\Sigma \setminus a$ is canonically identified (at least up to isotopy) with Σ_a^* and thus $\mathcal{M}(\Sigma \setminus a)$ is canonically isomorphic to $\mathcal{M}(\Sigma_a^*)$. Hence, we can define the *surgery homomorphism*

$$\sigma_a \colon \mathcal{M}(\Sigma, a) \to \mathcal{M}(\Sigma_a)$$

as the composition

$$\mathcal{M}(\Sigma, a) \xrightarrow[\mathrm{cut}_a]{} \mathcal{M}(\Sigma \setminus a) \xrightarrow[\cong]{} \mathcal{M}(\Sigma_a^*) \xrightarrow[\mathrm{forget}]{} \mathcal{M}(\Sigma_a), \qquad \mathcal{M}(\Sigma, a) \xrightarrow{\sigma_a} \mathcal{M}(\Sigma_a)$$

where the last map is induced by forgetting the marked points in Σ_a^*.

Applying this to surface diagram we obtain the following.

Lemma 4.5. *Let $\mathfrak{S} = (\Sigma; \gamma_1, \dots, \gamma_c)$ be a surface diagram. Then*

$$\tilde{\mu}_{\mathfrak{S}} := \tau_{\tau_{\gamma_c}(\gamma_1)} \circ \tau_{\tau_{\gamma_{c-1}}(\gamma_c)} \circ \tau_{\tau_{\gamma_1}(\gamma_2)} \in \mathcal{M}(\Sigma)$$

is contained in $\mathcal{M}(\Sigma, \gamma_1)$ and satisfies $\sigma_{\gamma_1}(\tilde{\mu}_{\mathfrak{S}}) = \mu_{\mathfrak{S}}$.

Proof. We claim that this follows from the observation that

$$\tau_{\tau_{\gamma_i}(\gamma_{i+1})}(\gamma_i) = \tau_{\gamma_i} \tau_{\gamma_{i+1}} \tau_{\gamma_i}^{-1}(\gamma_i) = \gamma_{i+1}.$$

[6]For a proof that cut_a is well defined see [I, Section 7.5], the rest follows as in [FM, Chapter 3].

Indeed, this obviously implies the first statement and the second follows from the fact that the diagrams

$$\begin{array}{ccccc} \Sigma & \longleftarrow & \Sigma \setminus \gamma_i & \longrightarrow & \Sigma^*_{\gamma_i} \\ \downarrow{\scriptstyle \tau_{\tau_{\gamma_i}(\gamma_{i+1})}} & & \downarrow & & \downarrow{\scriptstyle \kappa_{\gamma_i,\gamma_{i+1}}} \\ \Sigma & \longleftarrow & \Sigma \setminus \gamma_{i+1} & \longrightarrow & \Sigma^*_{\gamma_{i+1}} \end{array}$$

commute up to isotopy. □

The above makes it interesting to study the map σ_{γ_1} and its kernel.

Lemma 4.6. *Let $a \subset \Sigma$ be a non-separating simple closed curve. Then the group $\mathcal{M}(\Sigma, a)$ is generated by elements of the form τ_c where $i(a,c) = 0$ and $\Delta_{a,b} := (\tau_a \tau_b)^3$ where $i(a,b) = 1$.*

We will refer to the mapping classes $\Delta_{a,b}$ as Δ-*twists*.

Proof. It follows from the short exact sequence (4.1) that we can obtain a generating set for $\mathcal{M}(\Sigma, a)$ by lifting a generating set for $\mathcal{M}(\Sigma \setminus a)$ and adding the Dehn twist about a. As a generating set for $\mathcal{M}(\Sigma \setminus a)$ we can take the collection Dehn twists and so called *half-twists* about simple arcs connecting the two punctures. Then the Dehn twists in $\mathcal{M}(\Sigma \setminus a)$ have obvious lifts in $\mathcal{M}(\Sigma)$ and it is easy to see that each half-twist lifts to a Δ-twist. □

Corollary 4.7. *The kernel of the surgery homomorphism $\sigma_a \colon \mathcal{M}(S, a) \to \mathcal{M}(\Sigma_a)$ contains the Dehn twist about a and all Δ-twists involving a.*

The expert will have noticed that the mapping class $\tilde{\mu}_{\mathfrak{S}}$ in Lemma 4.5 is simply the monodromy of the boundary of the Lefschetz part of the simplified broken Lefschetz fibration obtained from $w_{\mathfrak{S}}$ by unsinking all the cusps. Of course, there are many different lifts of $\mu_{\mathfrak{S}}$ to $\mathcal{M}(\Sigma)$. For example, it follows from the braid relations for the pairs of adjacent curves that

$$\begin{aligned} \tilde{\mu}_{\mathfrak{S}} &= \tau_{\gamma_1}^{-c}(\tau_{\gamma_c}\tau_{\gamma_1})(\tau_{\gamma_{c-1}}\tau_{\gamma_c}) \dots (\tau_{\gamma_1}\tau_{\gamma_2}) \\ &= \tau_{\gamma_1}^{-2c}(\tau_{\gamma_c}\tau_{\gamma_1}\tau_{\gamma_c})(\tau_{\gamma_{c-1}}\tau_{\gamma_c}\tau_{\gamma_{c-1}}) \dots (\tau_{\gamma_1}\tau_{\gamma_2}\tau_{\gamma_1}) \end{aligned}$$

and since τ_{γ_1} is contained in the kernel of σ_{γ_1} we obtain two other choices.

We illustrate these mapping class group techniques to produce many examples of surface diagrams with trivial monodromy.

Example 4.8. Given an arbitrary circuit $\Gamma = (\gamma_1, \dots, \gamma_l)$ in an oriented surface Σ we can form a closed circuit $D\Gamma := (\gamma_1, \dots, \gamma_{l-1}, \gamma_l, \gamma_{l-1}, \dots, \gamma_2)$ which we call the *double* of Γ. We claim that the surface diagram $D\mathfrak{S} := (\Sigma, D\Gamma)$ has trivial monodromy. For convenience let us write $\tau_i = \tau_{\gamma_i}$. According to Remark **??** the monodromy of $D\mathfrak{S}$ can be lifted to $\mathcal{M}(\Sigma)$ as

$$\begin{aligned} \mu &= (\tau_2\tau_1\tau_2)\dots(\tau_{l-2}\tau_{l-1}\tau_{l-2})(\tau_{l-1}\tau_l\tau_{l-1})(\tau_l\tau_{l-1}\tau_l)(\tau_{l-1}\tau_{l-2}\tau_{l-1})\dots(\tau_1\tau_2\tau_1) \\ &= (\tau_2\tau_1\tau_2)\dots(\tau_{l-2}\tau_{l-1}\tau_{l-2})\Delta_{\gamma_{l-1},\gamma_l}(\tau_{l-1}\tau_{l-2}\tau_{l-1})\dots(\tau_1\tau_2\tau_1). \end{aligned}$$

Our goal is to factor this expression into a sequence of Δ-twists involving γ_1. The key observation is that

$$\begin{aligned} &(\tau_{l-2}\tau_{l-1}\tau_{l-2})\Delta_{\gamma_{l-1},\gamma_l}(\tau_{l-1}\tau_{l-2}\tau_{l-1}) \\ =&(\tau_{l-2}\tau_{l-1}\tau_{l-2})\Delta_{\gamma_{l-1},\gamma_l}(\tau_{l-2}\tau_{l-1}\tau_{l-2}) \\ =&(\tau_{l-2}\tau_{l-1}\tau_{l-2})\Delta_{\gamma_{l-1},\gamma_l}(\tau_{l-2}\tau_{l-1}\tau_{l-2})^{-1}\Delta_{\gamma_{l-2},\gamma_{l-1}} \\ =&\Delta_{\tau_{l-2}\tau_{l-1}\tau_{l-2}(\gamma_{l-1}),\tau_{l-2}\tau_{l-1}\tau_{l-2}(\gamma_l)}\Delta_{\gamma_{l-2},\gamma_{l-1}} \\ =&\Delta_{\gamma_{l-2},\tau_{l-2}\tau_{l-1}\tau_{l-2}(\gamma_l)}\Delta_{\gamma_{l-2},\gamma_{l-1}}. \end{aligned}$$

Applying this repeatedly we eventually obtain

$$\mu = \Delta_{\gamma_1,\delta_l}\Delta_{\gamma_1,\delta_{l-1}}\dots\Delta_{\gamma_1,\delta_2}$$

where $\delta_k := (\tau_1\tau_2\tau_1)\dots(\tau_{k-2}\tau_{k-1}\tau_{k-2})(\gamma_k)$. Hence, the monodromy of $D\mathfrak{S}$ is trivial by Corollary 4.7.

If Γ was a closed circuit to begin with so that $\mathfrak{S} = (\Sigma, \Gamma)$ is a surface diagram, then one can show that $Z_{D\mathfrak{S}}$ closes off to $DZ_{\mathfrak{S}} = Z_{\mathfrak{S}} \cup_\partial \overline{Z_{\mathfrak{S}}}$, the double of $Z_{\mathfrak{S}}$, whence the name.

4.2. **Drawing Kirby diagrams.** In this section we show how to translate surface diagrams into Kirby diagrams of the associated simple wrinkled fibrations. For the necessary background we refer the reader to [GS]. Throughout, we use Akbulut's *dotted circle notation* for 1-handles to avoid ambiguities for framing coefficients.

4.2.1. *Descending simple wrinkled fibrations.* Let $w\colon Z \to D^2$ be a descending simple wrinkled fibration of genus g with surface diagram $\mathfrak{S} = (\Sigma_g; \gamma_1, \dots, \gamma_c)$. Recall that the associated handle decomposition of Z is obtained from (some handle decomposition of) $\Sigma_g \times D^2$ by attaching 2-handles along $\gamma_i \subset \Sigma_g \times \{\theta_i\}$ with respect to the fiber framing where $\theta_1, \dots, \theta_c \in S^1$ are ordered according to the orientation on S^1. So in order to draw a Kirby diagram for Z we need to find a diagram for $\Sigma \times D^2$ in which the fibers of the boundary should be as clearly visible as possible.

A convenient choice is the diagram shown in Figure 10 which is induced from the obvious handle decomposition of Σ_g with one 0-handle, $2g$ 1-handles and one 2-handle. One fiber of $\Sigma_g \times S^1$, which we identify with Σ_g, is clearly visible and the canonical generators $a_1, b_1, \dots, a_g, b_g$ for $H_1(\Sigma_g)$ are also indicated. We have chosen the orientations such that $\langle a_i, b_i\rangle_{\Sigma_g} = 1$. Another advantage of this picture is that the fiber framing agrees with the blackboard framing. One minor drawback is that the picture does not immediately show *all* fibers of $\Sigma_g \times S^1$ but only an interval worth of them (just thicken the surface a little). However, this is actually enough for our purposes since we only need the fibers over the interval $[\theta_1, \theta_c] \subset S^1$. To get the orientations right we require that the orientation of the fiber agrees with the standard orientation of the plane and, according to the "fiber first convention", the positive S^1-direction points out of the plane.

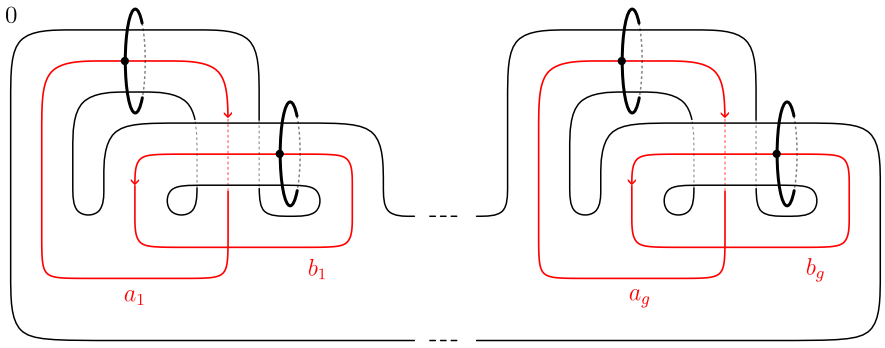

FIGURE 10. A diagram for $\Sigma_g \times D^2$ where fiber and blackboard framing agree. The red curves show a basis for $H_1(\Sigma_g)$.

With this understood, it is easy to locate the attaching curves of the fold handles in the diagram and it remains to determine their framing coefficients. More generally, we can describe the linking form of the link corresponding to the fold

handles. It should be no surprise that the framing and linking information in the diagram depends on our choice of the handle decomposition for Σ_g.

Let $\gamma \subset \Sigma_g$ be a simple closed curve. After choosing an orientation its homology class $[\gamma] \in H_1(\Sigma)$ can be expressed as

$$[\gamma] = \sum_{i=1}^{g} \big(n_{a_i}(\gamma)\, a_i + n_{b_i}(\gamma)\, b_i\big).$$

We identify Σ_g with $\Sigma_g \times \{0\}$ and, by a slight abuse of notation, we continue to denote the canonical push-off of γ to $\Sigma_g \times \{z\}$, $z \in D^2$, by γ.

Lemma 4.9. *For a simple closed curve $\gamma \subset \Sigma_g \times \{\theta\}$, $\theta \in [\theta_1, \theta_c] \subset S^1$, the framing coefficient of the fiber framing in Figure 10 is given by*

$$\mathrm{fr}(\gamma) = \sum_{i=1}^{g} n_{a_i}(\gamma) n_{b_i}(\gamma). \tag{4.2}$$

Furthermore, if $\gamma \subset \Sigma_g \times \{\theta\}$ and $\gamma' \subset \Sigma_g \times \{\theta'\}$, $\theta, \theta' \in [\theta_1, \theta_c]$, are two oriented simple closed curves, then their linking number in Figure 10 is

$$\begin{aligned} \mathrm{lk}(\gamma, \gamma') =& \frac{1}{2}\mathrm{sgn}(\theta - \theta')\big\langle \gamma, \gamma' \big\rangle \\ &+ \frac{1}{2} \sum_{i=1}^{g} \big[n_{a_i}(\gamma) n_{b_i}(\gamma') + n_{a_i}(\gamma') n_{b_i}(\gamma) \big] \end{aligned} \tag{4.3}$$

where $\langle \gamma, \gamma' \rangle$ is the algebraic intersection number of γ and γ' in Σ_g and sgn *denotes the sign of a real number*[7].

Proof. First observe that $\gamma \subset \Sigma_g \times \{\theta\}$ can be isotoped off the 2-handle to be completely visible in Figure 10 and, since the fiber framing and blackboard framing agree, its framing coefficient is given by its writhe in the diagram, i.e. the signed count of crossings with some chosen orientation. From the way the diagram is drawn it is clear that each crossing is caused by γ running over a_i *and* b_i for some i and that their signed sum is given by the right hand side of (4.2).

The statement about linking numbers follows from a similar count of crossings. Recall that the linking number of two oriented knots can be computed from any link diagram as half of the signed number of crossings. The second term on the right hand side of (4.3) arises just as above. However, the first term deserves some explanation. Each (transverse) intersection point of γ and γ' in Σ_g contributes a crossing in the diagram. Now, the sign of the crossing depends one two things: the sign of the intersection point and the information which strand is on top in the diagram. From Figure 11 we see that the contribution of each crossing is exactly as in (4.2). □

Remark 4.10. Formula 4.3 can be used to obtain a description of the intersection form of the 4-manifold $Z_{\mathfrak{S}}$ described by a surface diagram $\mathfrak{S}$ which only uses the data in $\mathfrak{S}$. Moreover, since 4.3 only depends on the homology classes of the curves in $\mathfrak{S}$, so do the intersection form and, in particular, the signature of $Z_{\mathfrak{S}}$. We will return to this observation in a future publication.

The diagrams of simple wrinkled fibrations derived from Figure 10 are good for abstract reasoning, however, in practice it is convenient to start with a cleaner diagram for $\Sigma_g \times D^2$ such as the one shown in Figure 12. In this picture, the fiber appears as the boundary sum of regular neighborhoods of the basis curves $\{a_i', b_i\}_{i=1}^{g}$ which, in turn, appear as meridians to the dotted circles. The framing coefficient of the fiber framing for simple closed curves on a fiber in Figure 12 can be computed

[7] To avoid any confusion, we use the convention that $\mathrm{sgn}(0) = 0$.

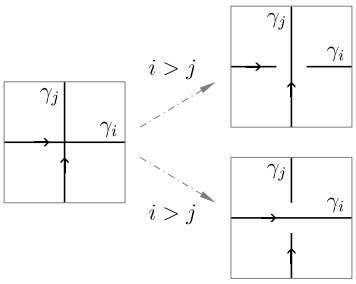

FIGURE 11. An intersection in a surface diagram and its crossing in the Kirby diagram.

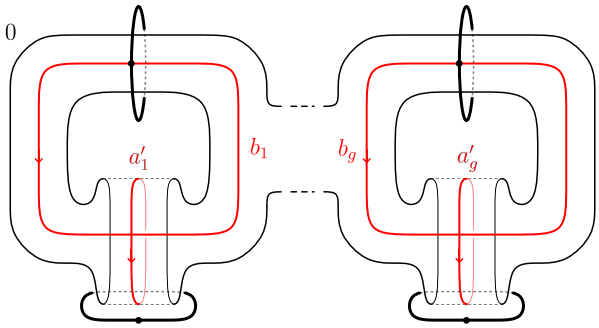

FIGURE 12. A cleaner diagram of $\Sigma_g \times D^2$.

as follows. It is not hard to see that Figure 12 is obtained from Figure 10 by a sequence of 1-handle slides and an isotopy of the 2-handle and vice versa. Note that these moves do not change the framing coefficients of any other 2-handles that might have been around. Moreover, during the moves, the b-curves remain fixed, while the a-curves undergo some changes. When pulling a'_i in Figure 12 back to Figure 10 one obtains a representative for the element

$$[a_1, b_1] * \cdots * [a_{i-1}, b_{i-1}] * a_i \in \pi_1(\Sigma_g)$$

where $[x, y] = xyx^{-1}y^{-1}$. The important observation is that while this curve is not isotopic to a_i it does represent the same homology class. As a consequence, formula (4.2) can be used for Figure 12 with a_i replaced by a'_i.

4.2.2. *Closing off and the last 2-handle.* Recall that our motivation comes from Williams' theorem that all closed, oriented 4-manifolds admit simple wrinkled fibrations over S^2. We have seen that these can be described (up to equivalence) by surface diagrams with trivial monodromy and we have already mentioned that it is in general not easy to check whether the monodromy of a given surface diagram is trivial. But the situation is even worse. Say that we know for some reason that a given surface diagram has trivial monodromy and let us also assume that the genus is at least three so that there are no gluing ambiguities. Even in this case it is not clear at all how the surface diagram encodes the information to complete the Kirby diagram.

To be more precise, let $w\colon X \to S^2$ be a simple wrinkled fibration with surface diagram $\mathfrak{S}$. Let $\nu\Sigma_-$ be a neighborhood of a lower genus fiber and let $Z := X \setminus \nu\Sigma_-$. Then w restricts to a descending simple wrinkled fibration on Z and ∂Z can be identified with $\Sigma_- \times S^1$ so that $\mathfrak{S}$ must have trivial monodromy. We can draw a

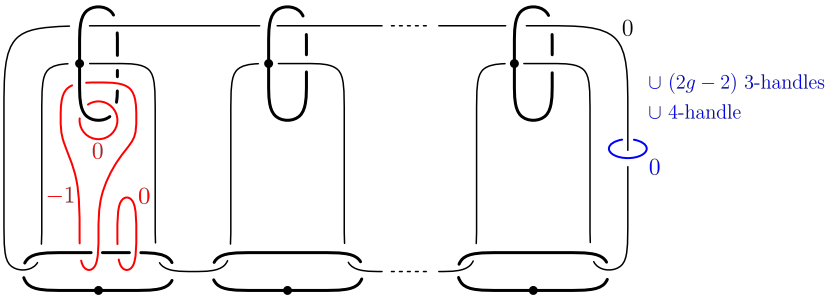

FIGURE 13. Manifolds with surface diagram $(\Sigma_g; a, \tau_b(a), b)$

Kirby diagram for Z as described in the previous section and to complete it to a diagram for X we have to understand how to glue $\nu\Sigma_-$ back in.

We can choose a handle decomposition for $\nu\Sigma_-$ with one 0-handle, $2g(\Sigma_-)$ 1-handles and one 2-handle. Turning this upside down results in a relative handle decomposition on $\partial Z \cong \Sigma_- \times S^1$ with one 2-handle, $2g(\Sigma_-)$ 3-handles and a 4-handle. The general theory tells us that the 3- and 4-handles attach in a standard way once we know how to attach the 2-handle. Unfortunately, it turns out to be rather difficult to locate this *last 2-handle* in the Kirby diagram for Z.

Our knowledge about the last 2-handle is a priori limited to the following observation. If we identify $\nu\Sigma_-$ with $\Sigma_- \times D^2$, then the attaching curve of the last 2-handle corresponds to $\{p\} \times \partial D^2$ for some $p \in \Sigma_-$. In particular, we see that it must be attached along a section of the boundary fibration $(\partial Z, w)$.

Remark 4.11. Given a surface diagram $\mathfrak{S}$ with trivial monodromy, there is a general method for finding possible last 2-handles for $Z_{\mathfrak{S}}$ which is not very conceptual but still useful in some situations.[8] One considers a Kirby diagram for $Z_{\mathfrak{S}}$ as a surgery diagram for $\partial Z_{\mathfrak{S}}$ and performs (3-dimensional) Kirby moves until the fibration structure is clearly visible as $\Sigma_- \times S^1$. In such a diagram it is easy to locate the possible attaching curves for last 2-handles. One can then pull back these curves to the original diagram by undoing the moves and dragging the curves along.

Just as in the Lefschetz case, the situation becomes easier if one knows that $Z_{\mathfrak{S}}$ can be closed off to a fibration over S^2 which admits a section. The proof of the following lemma is the same as in the Lefschetz case and we refer the reader to [GS].

Lemma 4.12. *Let $w\colon X \to S^2$ be a simple wrinkled fibration with surface diagram $\mathfrak{S}$. If w admits a section of self-intersection k, then the last two handle appears in the diagram for $Z_{\mathfrak{S}}$ as a k-framed meridian of the 2-handle corresponding to the fiber. Furthermore, if $\mathfrak{S}$ is a surface diagram and a meridian as above can be used to attach the last 2-handle, then the corresponding simple wrinkled fibration admits a section of self-intersection k.*

In order to illustrate Remark 4.11 and Lemma 4.12 as well as our method of drawing Kirby diagrams we give an example which is also a warm up for the next section.

Example 4.13. Let $a, b \subset \Sigma_g$ be a geometrically dual pair of simple closed curves. We claim that $\mathfrak{S} = (\Sigma_g; a, \tau_b(a), b)$ is a surface diagram for $\Sigma_{g-1} \times S^2 \# \overline{\mathbb{C}P^2}$. We can assume that a and b are the standard generators a_1 and b_1 in Figure 12 and Figure 13 shows the final Kirby diagram. In order to see how we got there let us first ignore all the blue components. What is left is just the Kirby diagram for $Z_{\mathfrak{S}}$. The

[8] Compare Chapter 8.2 in [GS] (p. 299f) for the Lefschetz case.

framings on the fold handles can either be computed using Lemma 4.9 (together with Proposition 2.6) or by hand[9]. We now perform the obvious handle moves: using the meridians to the two 1-handles on the left we first unlink the -1-framed fold handle (corresponding to $\tau_b(a)$) to obtain a -1-framed unknot isolated from the rest of the diagram, then we unlink the black 2-handle (corresponding to the fiber) and finally cancel the 1-handles and their meridians. Obviously, the thus obtained diagram shows $\Sigma_{g-1} \times D^2 \# \overline{\mathbb{C}P^2}$ and the boundary is clearly visible as $\Sigma_{g-1} \times S^1$. Moreover, it is easy to see that the last 2-handle can be attached along a 0-framed meridian to the fiber 2-handle and the resulting manifold is $\Sigma_{g-1} \times S^2 \# \overline{\mathbb{C}P^2}$ as claimed. Finally, since we attached the last 2-handle in a region that was not affected by the Kirby moves it will not change when we undo the moves again and we arrive at Figure 13. Lemma 4.12 then tells us that the corresponding simple wrinkled fibration will have a section of self-intersection zero.

Note that for $g \geq 3$ the way we have attached the last 2-handle is unique. In the lower genus cases there are more options. However, in any case one will end up with a blow-up of some surface bundle over S^2.

4.3. **Relation to broken Lefschetz fibrations.** Let $w\colon X \to B$ be a simple wrinkled fibration. After trading all the cusps for Lefschetz singularities by applying Lekili's unsinking modification we obtain a broken Lefschetz fibration

$$\beta_w\colon X \to B$$

with one round singularity, smoothly embedded in the base, and all its Lefschetz points on the higher genus side. If the base is the sphere or the disk, then β_w is a *simplified broken Lefschetz fibration* in the sense of [B2] and thus induces another handle decomposition of X.

In order to relate these two handle decompositions, let us briefly review how a handle decomposition is obtained from a simplified broken Lefschetz fibration $\beta\colon X \to B$. Much in the spirit of simple wrinkled fibrations one chooses a reference point in the higher genus region together with a collection of disjointly embedded arcs $L_1, \dots, L_k, R \subset B$, where k is the number of Lefschetz singularities, emanating from the reference point such that each L_i ends in a Lefschetz point and R passes through the round singularity once. Such a system of arcs is known as a *Hurwitz system* for β. The arcs in a Hurwitz system then give rise to simple closed curves in the reference fiber Σ to which we shall refer to as the *Lefschetz vanishing cycles* $\lambda_1, \dots, \lambda_k \subset \Sigma$ and the *round vanishing cycle* ρ. A handle decomposition of X is then given as follows:

- Start with $\Sigma \times D^2$
- Going around S^1 attach a *Lefschetz handle* along the λ_i pushed off into fibers over S^1, i.e. 2-handles with framing -1 with respect to the fiber framing
- Attach a *round 2-handle* along ρ

The round 2-handle decomposes into a 2-handle and a 3-handle such that the 3-handle goes over the 2-handle geometrically twice and the 2-handle is attached along ρ with respect to the fiber framing. (For more details see [B2].)

Now let $w\colon X \to B$ be a simple wrinkled fibration and let β_w be the associated simplified broken Lefschetz fibration. Given a reference system $\mathcal{R} = \{R_i\}$ for w with associated surface diagram (Σ, Γ) there is a canonical Hurwitz system for β_w. Since the unsinking homotopy is supported near the cusps we can assume that the nothing happens around the reference paths. Now observe that the arcs R_i cut

[9]The curve is simple enough to draw a parallel push-off in the fiber direction and compute the linking number

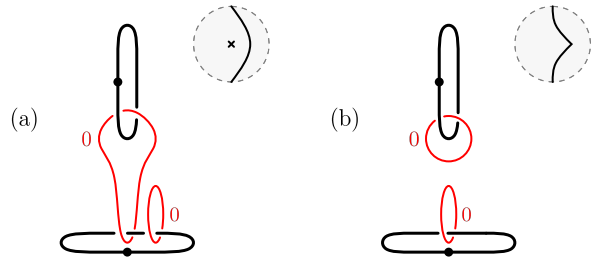

FIGURE 14. A Lefschetz singularity (a) before and (b) after sinking.

the higher genus region into triangles each containing a single Lefschetz singularity of β_w. Thus, up to isotopy, there is a unique arc L_i in the triangle bounded by R_i and R_{i+1} going from the reference fiber to the Lefschetz singularity and for the round singularity we take the arc $R = R_1$. According to Lekili [L], the vanishing cycles of β_w with respect to this Hurwitz system are given by

$$\lambda_i = \tau_{\gamma_i}(\gamma_{i+1}) \quad \text{and} \quad \rho = \gamma_1.$$

We can go from the handle decomposition induced by β_w to the one induced by w using the following handlebody interpretation of the (un-)sinking deformation.

Assume that we have a Lefschetz singularity next to a fold arc that is *sinkable*, i.e. the Lefschetz and fold vanishing cycles intersect in one point. (In other words, it is the resulting of unsinking a cusp.) In terms of handle decompositions the situation before and after the sinking process is locally described in Figure 14.[10] (The Lefschetz 2-handle in (a) is the one that goes over both 1-handles. One readily checks that it is correctly framed.) Clearly, both pictures describe a 4-ball and they are related by an obvious 2-handle slide. Indeed, to go from (a) to (b) one has to slide the Lefschetz handle over the fold handle in such a way that it unlinks from the lower 1-handle. Note that his handle slide is compatible with the fibration structures in the sense that the attaching curves stay on the fibers. Moreover, it mysteriously adjusts the framings exactly as needed.

Remark 4.14. Although the handle slide described above seems to be a correct interpretation of Lekili's (un-)sinking deformation it is a priori not obvious why this should be true. In fact, the deformation is a combination of wrinkling, merging and flipping (see [L], Figure 8) and does not seem very atomic. On the other hand, the handle slide is an atomic modification of the handlebodies. It would be interesting to see a 1-parameter family of Morse functions associated with the (un-)sinking deformation that would exhibit the handle slide.

This shows that, if we start we the handle decomposition of β_w, then sliding λ_1 over $\rho = \gamma_1$ produces a fiber framed attaching curve λ_1' which is isotopic to γ_2. Successively sliding λ_i over $\lambda_{i-1}' \sim \gamma_i$ results in fiber framed attaching curves λ_i' isotopic to γ_{i+1}. Altogether we end up with fiber framed curves $\lambda_1', \dots, \lambda_c', \rho$. The final observation is that λ_c' is isotopic to $\rho = \gamma_1$ and can be unlinked and isolated from the rest of the diagram to form a zero framed unknot which cancels the 3-handle coming from the round singularity. What we are left with is the decomposition associated to w.

5. SUBSTITUTIONS

Let $\mathfrak{S} = (\Sigma, \Gamma)$ be a surface diagram and let Λ be a subcircuit of Γ. If Λ' is any circuit that starts and ends with the same curves as Λ, then we can build a new

[10] These handle decompositions have already appeared in a disguised form in [L].

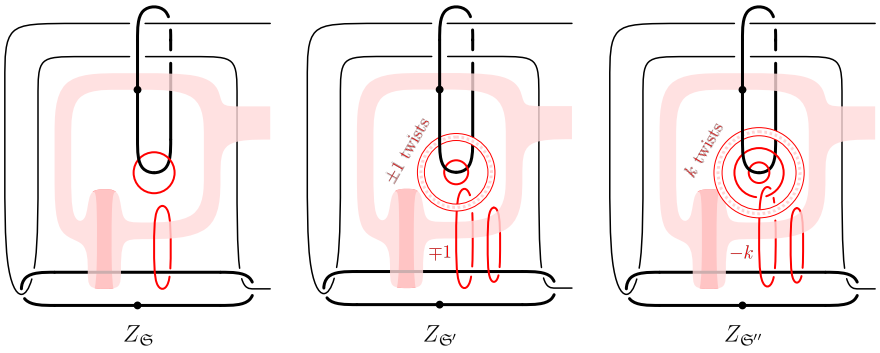

FIGURE 15. The relevant parts of the handle decompositions of $Z_{\mathfrak{S}}$, $Z_{\mathfrak{S}'}$ and $Z_{\mathfrak{S}''}$. All 2-handles without framing coefficient are 0-framed.

surface diagram (Σ, Γ') where Γ' is obtained by replacing Λ with Λ'. We call this operation a *substitution of type* $(\Lambda|\Lambda')$[11].

Passing to the associated simple wrinkled fibrations one can ask how such a substitution affects the total spaces. In the following we will treat two instances in which this question can be answered. Our main tool are the handle decompositions exhibited in the previous section.

Let Z be a compact 4-manifold, possibly with nonempty boundary. Recall that the *blow-up* of Z is the connected sum of Z with either $\overline{\mathbb{C}P^2}$ or $\mathbb{C}P^2$ (taken in the interior of Z). Moreover, the *sum stabilization* of Z usually means the connected sum with $S^2 \times S^2$. We will be slightly more general and also allow connected sums with $\mathbb{C}P^2 \# \overline{\mathbb{C}P^2}$, the twisted S^2-bundle over S^2. For convenience, we let

$$\mathbb{S}_k := \begin{cases} S^2 \times S^2, & k \text{ even} \\ \mathbb{C}P^2 \# \overline{\mathbb{C}P^2}, & k \text{ odd} \end{cases}$$

and note that $\mathbb{S}_k$ is described by the $(0,k)$-framed Hopf link.

Lemma 5.1 (Blow-ups and sum stabilizations)**.** *Let $\mathfrak{S} = (\Sigma, \Gamma)$ be a surface diagram and let $\mathfrak{S}'$ be obtained from $\mathfrak{S}$ by a substitution of type*

$$\big(a, b \,|\, a, \tau_b^{\pm 1}(a), b\big). \tag{5.1}$$

Furthermore, let $\mathfrak{S}''$ be obtained by a substitution of type

$$\big(a, b \,|\, a, b, \tau_b^{k}(a), b\big). \tag{5.2}$$

Then $Z_{\mathfrak{S}'}$ is diffeomorphic to the blow-up $Z_{\mathfrak{S}} \# \mp \mathbb{C}P^2$ and $Z_{\mathfrak{S}''}$ is diffeomorphic to the sum stabilization $Z_{\mathfrak{S}} \# \mathbb{S}_{-k}$.

Of course, any substitution is reversible so that whenever a surface diagram contains a configuration of the form $(a, \tau_b^{\pm 1}(a), b)$ or $(a, b, \tau_b^k(a), b)$ the associated 4-manifold must be a blow-up or sum stabilization, respectively. We will call these *blow-up* (resp. *sum stabilization*) *configurations*.

Proof. By switching we can assume that $\Gamma = (\dots, a, b)$ and thus $\Gamma'(\dots, a, \tau_b^{\pm 1}(a), b)$ and $\Gamma'' = (\dots, a, b, \tau_b^k(a), b)$. Figure 15 shows the relevant parts of the handle decompositions of the associated 4-manifolds. The shaded ribbons indicate the regions that contain all the other fold handles. Note that the curves a and b appear as 0-framed meridians to the dotted circles.

[11]Similar substitution techniques for Lefschetz fibrations are studied in [EG, EMVHM].

In the case of $Z_{\mathfrak{S}'}$ we can use the meridians to unlink the curve corresponding to $\tau_b^{\pm}(a)$ resulting in an unknot with framing ∓ 1 which is isolated from the rest of the diagram. Furthermore, the rest of the diagram agrees with the diagram for $Z_{\mathfrak{S}}$ and the claim follows.

The argument for $Z_{\mathfrak{S}''}$ is almost the same. Again, by sliding over the meridians we can isolate the curves corresponding to b and $\tau_b^k(a)$ from the rest of the diagram. This time we obtain a $(0,-k)$-framed Hopf link which represents a copy of $\mathbb{S}_{-k}$. □

Proposition 5.2. *Let $\mathfrak{S}$, $\mathfrak{S}'$ and $\mathfrak{S}''$ be as in Lemma 5.1.*

1. *All three diagrams have the same monodromy.*
2. *If $\mathfrak{S}$ has trivial monodromy so that $Z_{\mathfrak{S}}$ closes off to a closed 4-manifold X, then $Z_{\mathfrak{S}'}$ (resp. $Z_{\mathfrak{S}'}$) closes off to $X \# \mp \mathbb{C}P^2$ (resp. $X \# \mathbb{S}_k$).*
3. *Any closed 4-manifold obtained from $\mathfrak{S}'$ (resp. $\mathfrak{S}''$) is a blow-up (resp. sum-stabilization) of a manifold obtained from $\mathfrak{S}$.*

Proof. The first statement follows directly from Lemma 5.1 since connected sums with closed manifold (taken in the interior) do not change the boundary.

For the other statements, observe that if one knows how to apply the method from Remark 4.11 for $\mathfrak{S}$, then one also knows it for $\mathfrak{S}'$ (resp. $\mathfrak{S}''$) and vice versa. □

Another instance where a substitution corresponds to a well known cut-and-paste operation has been observed by Hayano ([H2], Lemma 6.13). Assume that a surface diagram $\mathfrak{S}$ contains a curve $c \subset \Sigma$. If $d \subset \Sigma$ is geometrically dual to c, then one can perform a substitution of type $(c|c,d,c)$ and Hayano shows that if $\mathfrak{S}'$ denotes the resulting surface diagram, then $Z_{\mathfrak{S}'}$ is obtained from $Z_{\mathfrak{S}}$ by a surgery on the curve $\delta \subset \Sigma \subset Z_{\mathfrak{S}}$ with respect to its *fiber framing*, i.e. the framing induced by the its canonical framing in Σ together with the framing of Σ in $Z_{\mathfrak{S}}$ as a regular fiber of $w_{\mathfrak{S}} \colon Z_{\mathfrak{S}} \to D^2$.

One immediately notices that our sum-stabilization substitution is a special case of this construction. However, it also leads the way to the following minor generalization of the surgery substitution which captures not only the fiber framed surgery but also the one with the opposite framing.

Lemma 5.3. *Let $\mathfrak{S}$ and $\mathfrak{S}'$ be two surface diagram with the same underlying surface Σ and let $c, d \subset \Sigma$ be a geometrically dual pair of simple closed curves. If $\mathfrak{S}'$ is obtained from $\mathfrak{S}$ by a substitution of type $(c|c, \tau_c^k(d), c)$, then $Z_{\mathfrak{S}'}$ is obtained from $Z_{\mathfrak{S}}$ by a surgery on $d \subset \Sigma \subset X$ with respect to the fiber framing when k is even and the opposite framing when k is odd.*

Proof. As in Hayano's proof, it is enough to work in a neighborhood of $c \cup d$ which we can assume to be a punctured torus. Using our handle decomposition instead of the ones from broken Lefschetz fibrations, the effect of Hayano's surgery substitution, i.e. the case when $k = 0$, looks as in Figure 16 where c (resp. d) appears as the meridian of the upper (resp. lower) 1-handle. To obtain the other even cases, observe that in Figure 16(b) we can slide the 2-handle corresponding to d once over each 2-handle corresponding to c in the same direction. Depending on the direction this changes the framing coefficient by ± 2 and one readily checks that the resulting curve diagram shows a neighborhood with vanishing cycles $(c, \tau_c^{\mp 2}(d), c)$. Repeating this trick one can obtain all configurations with even k and they will all describe the fiber framed surgery on d.

As shown in [GS, Example 8.4.6] the surgery with the opposite framing can be realized by inserting a pair of a Lefschetz vanishing cycle and an achiral Lefschetz vanishing cycle which are both parallel to d. But Figure 17 shows that the result is the same as a substitution of type $(c|c, \tau_c^{-1}(d), c)$ which corresponds to $k = -1$. Moreover, the arguments for shifting the value of k by multiple of 2 works just as

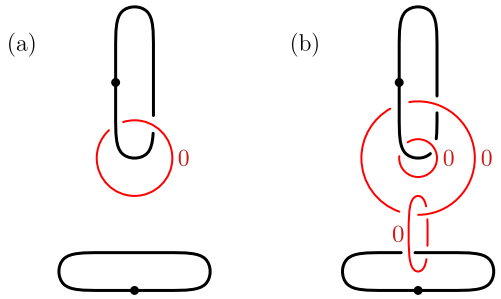

FIGURE 16. Hayano's surgery substitution: neighborhoods with (a) vanishing cycle c and (b) vanishing cycles (c, d, c).

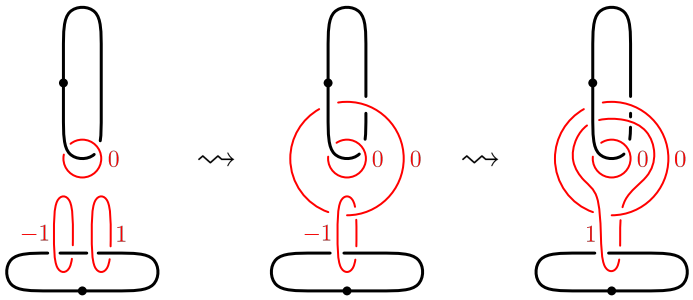

FIGURE 17. Surgery with the opposite framing.

in the fiber framed case. □

Using the above lemma the sum-stabilization can be interpreted as performing surgery on a null-homotopic curve with either of its framing. Indeed, as d one takes one of the adjacent vanishing cycles of c in $\mathfrak{S}$ which is clearly null-homotopic in $Z_{\mathfrak{S}}$.

It would be interesting to interpret other cut-and-paste operations on 4-manifolds as substitutions in surface diagrams. For example, it is reasonable to expect such an interpretation for certain rational blow downs which can be described in terms of Lefschetz fibrations (see [EMVHM]). However, we will settle for blow-ups and sum-stabilizations in this paper.

6. Manifolds with genus 1 simple wrinkled fibrations

In this section we prove Theorem 1.1. Our strategy is to use Proposition 5.2 to construct some genus 1 simple wrinkled fibrations and then show that this construction gives all such fibrations.

We begin with the construction of genus 1 simple wrinkled fibrations over S^2. As before, we denote by $\mathbb{S}_k$ the closed 4-manifolds described by the $(0, k)$-framed Hopf link and we define a family of manifolds

$$X_{klmn} = \mathbb{S}_k \# l(S^2 \times S^2) \# m\mathbb{C}P^2 \# n\overline{\mathbb{C}P^2}, \quad k \in \{0, 1\}\,, \ l, m, n \geq 0. \tag{6.1}$$

Note that these are precisely the manifolds in Theorem 1.1. Recall that $\mathbb{S}_k$ is an S^2-bundle over S^2. By performing a birth on a suitable bundle projection $\mathbb{S}_k \to S^2$ we obtain a simple wrinkled fibration with two cusps. We can then use Lemma 5.1 to add the other summands at will. Thus, in order to prove Theorem 1.1, it remains to show the following.

Proposition 6.1. *Let $w\colon X \to S^2$ be a simple wrinkled fibration of genus 1. Then X is diffeomorphic to some X_{klmn} described in* (6.1).

Remark 6.2. The reason for our small reformulation of Theorem 1.1 is that, while the original formulation is cleaner, the new one is much more in tune with the structure of the proof.

The key to the proof of Proposition 6.1 is the simple nature of simple closed curves on the torus. Indeed, the two well known facts that two oriented simple closed curves on the torus are isotopic if and only if they are homologous and that the (absolute value of the) algebraic and geometric intersection numbers agree allow us to transfer the whole discussion of genus 1 surface diagrams into the homology group $H_1(T^2) \cong \mathbb{Z} \oplus \mathbb{Z}$ simply by choosing orientations on the curves. Building on this observation we obtain the following result about the structure of genus 1 surface diagrams.

Lemma 6.3. *Any closed circuit on the torus of length at least three contains blow-up or sum stabilization configurations (as described in Lemma 5.1).*

Proof. Let $\Gamma = (\gamma_1, \dots, \gamma_c)$ be a (not necessarily closed) circuit on the torus of length $c \geq 3$. As usual, we choose an arbitrary orientation on γ_1 and orient the remaining curves by requiring that $\langle \gamma_i, \gamma_{i+1} \rangle = 1$ for $i < c$ so that we can consider each γ_i as an element of $H_1(T^2)$.

We first observe that, since any two adjacent curves in Γ algebraically dual, they form a basis of $H_1(T^2)$. In particular, for $i \geq 3$ we can write

$$\gamma_i = k_i \gamma_{i-1} - \gamma_{i-2}, \quad k_i \in \mathbb{Z}$$

where the coefficient of γ_{i-2} determined by our convention that $\langle \gamma_{i-1}, \gamma_i \rangle = 1$. This shows that if we denote by $\sigma_i := \langle \gamma_1, \gamma_i \rangle$ the algebraic intersection number between γ_1 and γ_i, then we have $\sigma_1 = 0$, $\sigma_2 = 1$ and the recursion formula

$$\sigma_i = k_i \sigma_{i-1} - \sigma_{i-2} \tag{6.2}$$

holds for $i \geq 3$. At this point we note that Γ is closed if and only if $|\sigma_c| = 1$.

We claim that if $|k_i| \geq 2$ for all $i \geq 3$, then $|\sigma_{i+1}| > |\sigma_{i+1}|$ for all i. This follows inductively since $|\sigma_2| > |\sigma_1|$ and from (6.2) we get

$$\begin{aligned} |\sigma_{i+1}| &= |k_{i+1}\sigma_i - \sigma_{i-1}| \\ &\geq \big| |k_{i+1}||\sigma_i| - |\sigma_{i-1}| \big| \\ &= |k_{i+1}||\sigma_i| - |\sigma_{i-1}| > |\sigma_i| \end{aligned}$$

where we have used the reverse triangle inequality, the induction hypothesis and the assumption that $|k_{i+1}| \geq 2$. As a consequence, we see that if Γ is closed, then we must have $|k_i| \leq 1$ for some $i \geq 3$.

Assume first that $k_i = \pm 1$. For the sake of a cleaner notation we momentarily rename the relevant curves to

$$(\gamma_{i-2}, \gamma_{i-1}, \gamma_i) =: (a, \xi, b). \tag{6.3}$$

By assumption, we have $b = \pm\xi - a$ and thus $\xi = \pm(a + b)$ and the orientation convention shows that $\langle a, b \rangle = \pm 1$. By invoking the Picard-Lefschetz formula (Proposition 2.6) we obtain

$$\begin{aligned} \tau_a^{\pm 1}(b) &= b \pm \langle a, b \rangle a \\ &= a + b \\ &= \pm\xi \end{aligned}$$

which, after forgetting the orientations again, reveals the excerpt of Γ shown in (6.3) as a blow-up configuration.

A similar argument exhibits a sum-stabilization configuration in the remaining case when $k_i = 0$. The details are left to the reader. □

The proof of Proposition 6.1, and thus of Theorem 1.1 is now very easy.

Proof of Proposition 6.1. Any genus one simple wrinkled fibration over S^2 can is obtained by closing off a manifold $Z_{\mathfrak{S}}$ associated to a surface diagram $\mathfrak{S} = (T^2, \Gamma)$. Moreover, any such diagram $\mathfrak{S}$ can be closed off since the mapping class group of the lower genus fiber is trivial. By Lemma 6.3 and Proposition 5.2 (3) we can successively split off summands of the form $\pm\mathbb{C}P^2$ and $\mathbb{S}_k$ until the remaining surface diagram, say $\mathfrak{S}_0$ has a circuit of length two. It is easy to see that $Z_{\mathfrak{S}_0}$ is the trivial disk bundle $S^2 \times D^2$. (Either by drawing a Kirby diagram or by observing that any simple wrinkled fibration with two cusps is homotopic to a bundle projection.) Thus there are exactly two ways to close off the fibration, producing a summand of the form $\mathbb{S}_0 \cong S^2 \times S^2$ or $\mathbb{S}_1 \cong \mathbb{C}P^2 \# \overline{\mathbb{C}P^2}$. □

7. Concluding remarks

The theory of simple wrinkled fibrations and surface diagrams is still in a very early stage and at this point it raises more questions then it provides answers. We would like to take the opportunity to point out some of the major problems in the subject as well as to indicate some further developments.

7.1. **Closed 4-manifolds.** The ultimate goal is to use surface diagrams to study *closed* 4-manifolds. Unfortunately, it turns out that most surface diagrams do *not* describe closed manifolds since they have non-trivial monodromy and it is usually a hard problem to determine whether a given surface diagram has trivial monodromy. The following is thus of great interest.

Problem 7.1. *Find at least necessary conditions for a surface diagram to have trivial monodromy that are easier to check.*

The next major problem was already mentioned in Section 4.2.2. If a surface diagram of sufficiently high genus is known to have trivial monodromy, then it determines a unique closed 4-manifold together with a simple wrinkled fibration over S^2 by closing off the associated fibration over the disk. However, the way that the surface diagram encodes the closing off information is too implicit for practical purposes. For example, by simply looking at the surface diagram it not at all clear how to answer the following very reasonable questions about the corresponding simple wrinkled fibration over S^2:

- Does the fibration have a section?
- What can be said about the homology class of the fiber? (Is it trivial, primitive, torsion,... ?)
- What is the fundamental group, homology, etc. of the total space?

What is missing is one more piece of information which is roughly the (framed) attaching curve of the last 2-handle. One can reformulate this issue in terms of mapping class groups (see [H2], for example)

Problem 7.2. *Find a practical method to determine the missing piece of information from a surface diagram with trivial monodromy.*

7.2. **Higher genus fibrations.** The fact that any (achiral) Lefschetz fibration can be turned into a simple wrinkled fibration of one genus higher suggests the philosophy that simple wrinkled fibrations of a fixed genus might behave similarly as (achiral) Lefschetz fibrations of one genus lower.

This analogy works rather well for the lowest possible fiber genera. Indeed, our result about genus one simple wrinkled fibrations looks very similar to the (rather trivial) classification of genus zero (achiral) Lefschetz fibrations, the latter being blow-ups of either $S^2 \times S^2$ or $\mathbb{C}P^2 \# \overline{\mathbb{C}P^2}$.

Following this train of thought one might hope to be able to say something useful about the classification of genus two simple wrinkled fibrations over S^2 but one should expect to be lost as soon as the genus is three or higher. However, it is nonetheless conceivable that part of the classification scheme that worked in the genus one case might carry over to higher genus fibrations, as we will now explain

Let $\mathfrak{S} = (\Sigma; \gamma_1, \dots, \gamma_l)$ be a surface diagram and assume that for some $2 < k < l$ the curve γ_k is geometrically dual to γ_1. Then there is an obvious way to decompose $\mathfrak{S}$ into the two smaller surface diagrams $(\Sigma; \gamma_1, \dots, \gamma_k)$ and $(\Sigma; \gamma_1, \gamma_k, \dots, \gamma_l)$. Repeating this process we eventually obtain a decomposition of $\mathfrak{S}$ into a collection of surface diagram with the property that no pair of non-adjacent curves has geometric intersection number one. Let us call such a surface diagram *irreducible*.

In terms of the simple wrinkled fibration associated to $\mathfrak{S}$ the above decomposition of $\mathfrak{S}$ should correspond to merging the fold arcs that induce γ_1 and γ_k. The result is a wrinkled fibration that naturally decomposes as a *boundary fiber sum* of the two simple wrinkled fibrations associated to the parts of the decomposition of $\mathfrak{S}$.

This suggests that any descending simple wrinkled fibration over the disk naturally decomposes into a boundary fiber sum of *irreducible* fibrations where we call a simple wrinkled fibration irreducible if its surface diagram is irreducible. Consequently, the classification of descending simple wrinkled fibrations splits into two parts: the classification of irreducible fibrations and understanding the effect of boundary fiber sums.

The genus one classification fits into this scheme as follows. Our arguments show that the only irreducible surface diagrams of genus one are given by the blow-up configurations $(a, \tau_a^{\pm 1}(b), b)$ and the sum-stabilization configurations $(a, b, \tau_b^k(a), b)$ for $k \neq 1$. Using the handle decompositions it is easy to identify the corresponding manifolds. (They are the connected sum of $S^2 \times D^2$ with either $\pm\mathbb{C}P^2$, $S^2 \times S^2$ or $\mathbb{C}P^2 \# \overline{\mathbb{C}P^2}$.) Furthermore, the boundary fiber sums are performed along spheres and are thus easy to understand.

Making these arguments precise requires an understanding of the effect of merging folds and cusps on surface diagrams.

7.3. **Uniqueness of surface diagrams.** Given the fact that all closed 4-manifolds can be described by surface diagrams, it is natural to ask for a set of moves to relate different surface diagrams that describe the same manifold, similar to the situation of 3-manifolds and Heegaard diagrams.

A first step in this direction was taken by Williams [W2] who relates the surface diagrams of homotopic simple wrinkled fibrations over S^2 of genus at least three. He shows that any two homotopic simple wrinkled fibrations can be connected by a special homotopy that is made up of four basic building blocks. These building blocks are simple enough to understand their effect on the initial surface diagram (see also the recent work of Hayano [H2]).

So far this is completely analogous to the 3-dimensional context. A new phenomenon in the 4-dimensional context is that two simple wrinkled fibrations on a given 4-manifold are not necessarily homotopic. The structure of the set $\pi^2(X) := [X, S^2]$ of homotopy classes of maps from a closed 4-manifold to the 2-sphere – also known as the *second cohomotopy set* of X – is described in [KMT] (see also the references therein). Our results show that an equivalence class of surface diagrams for X determines an orbit of the action of the diffeomorphism group of X on $\pi^2(X)$. This action is usually neither trivial[12] nor transitive[13]. Consequently, reparametrizing a

[12]For example the diffeomorphism of $S^2 \times S^2$ that interchanges the two factors also interchanges the projections onto the factors which are easily seen not to be homotopic.

[13]This follows from the fact that the diffeomorphism action on $H_2(X)$ preserves divisibility.

surface diagram can change the homotopy class of its simple wrinkled fibration but one cannot expect to obtain all homotopy classes in this way.

A general method for relating broken fibrations in different homotopy classes is the *projection move* mentioned in [W1] but it is not at all obvious how to interpret this procedure in terms of surface diagrams. Altogether, the problem of relating surface diagram with non-homotopic fibrations is still wide open.

References

[AK] Selman Akbulut and Çağrı Karakurt, *Every 4-manifold is BLF*, J. Gökova Geom. Topol. GGT **2** (2008), 83–106. MR2466002 (2009k:57037)

[ADK] Denis Auroux, Simon K. Donaldson, and Ludmil Katzarkov, *Singular Lefschetz pencils*, Geom. Topol. **9** (2005), 1043–1114 (electronic), DOI 10.2140/gt.2005.9.1043. MR2140998 (2005m:53164)

[B1] R. İnanç Baykur, *Existence of broken Lefschetz fibrations*, Int. Math. Res. Not. IMRN (2008), Art. ID rnn 101, 15. MR2439543 (2010b:57026)

[B2] Refik İnanç Baykur, *Topology of broken Lefschetz fibrations and near-symplectic four-manifolds*, Pacific J. Math. **240** (2009), no. 2, 201–230, DOI 10.2140/pjm.2009.240.201. MR2485463 (2010c:57035)

[BK] Refik İnanç Baykur and Seiichi Kamada, *Classification of broken Lefschetz fibrations with small fiber genera* (2010), available at `http://de.arxiv.org/abs/1010.5814v2`.

[D] S. K. Donaldson, *Lefschetz pencils on symplectic manifolds*, J. Differential Geom. **53** (1999), no. 2, 205–236. MR1802722 (2002g:53154)

[EE] Clifford J. Earle and James Eells, *A fibre bundle description of Teichmüller theory*, J. Differential Geometry **3** (1969), 19–43. MR0276999 (43 #2737a)

[EG] Hisaaki Endo and Yusuf Z. Gurtas, *Lantern relations and rational blowdowns*, Proc. Amer. Math. Soc. **138** (2010), no. 3, 1131–1142, DOI 10.1090/S0002-9939-09-10128-4. MR2566578 (2011a:57047)

[EMVHM] Hisaaki Endo, Thomas E. Mark, and Jeremy Van Horn-Morris, *Monodromy substitutions and rational blowdowns*, J. Topol. **4** (2011), no. 1, 227–253, DOI 10.1112/jtopol/jtq041. MR2783383

[FM] Benson Farb and Dan Margalit, *A Primer on Mapping Class Groups*, Princeton Mathematical Series, vol. 49, Princeton University Press, Providence, RI, 2011.

[GK1] David T. Gay and Robion Kirby, *Constructing Lefschetz-type fibrations on four-manifolds*, Geom. Topol. **11** (2007), 2075–2115, DOI 10.2140/gt.2007.11.2075. MR2350472 (2009b:57048)

[GK2] ———, *Indefinite Morse 2-functions; broken fibrations and generalizations* (2011), available at `arXiv:1102.0750v2[math.GT]`.

[GK3] ———, *Fiber connected, indefinite Morse 2-functions on connected n-manifolds* (2011), available at `arXiv:1102.2169v2[math.GT]`.

[GK4] ———, *Reconstructing 4-manifolds from Morse 2-functions* (2012), available at `http://de.arxiv.org/abs/1202.3487`.

[GG] M. Golubitsky and V. Guillemin, *Stable mappings and their singularities*, Springer-Verlag, New York, 1973. Graduate Texts in Mathematics, Vol. 14. MR0341518 (49 #6269)

[GS] Robert E. Gompf and András I. Stipsicz, *4-manifolds and Kirby calculus*, Graduate Studies in Mathematics, vol. 20, American Mathematical Society, Providence, RI, 1999. MR1707327 (2000h:57038)

[H1] Kenta Hayano, *On genus 1 simplified broken Lefschetz fibrations*, Alg. Geom. Topol. **11** (2011), no. 3, 1267–1322, DOI 10.2140/agt.2011.11.1267.

[H2] ———, *Modification rule of monodromies in R_2-move* (2012), available at `http://de.arxiv.org/abs/1203.4299v1`.

[I] Nikolai V. Ivanov, *Subgroups of Teichmüller modular groups*, Translations of Mathematical Monographs, vol. 115, American Mathematical Society, Providence, RI, 1992. Translated from the Russian by E. J. F. Primrose and revised by the author. MR1195787 (93k:57031)

[K] A. Kas, *On the handlebody decomposition associated to a Lefschetz fibration*, Pacific J. Math. **89** (1980), no. 1, 89–104. MR596919 (82f:57012)

[KMT] Robion Kirby, Paul Melvin, and Peter Teichner, *Cohomotopy sets of 4-manifolds* (2012), available at `http://de.arxiv.org/abs/1203.1608v1`.

[L] Yanki Lekili, *Wrinkled fibrations on near-symplectic manifolds*, Geom. Topol. **13** (2009), no. 1, 277–318, DOI 10.2140/gt.2009.13.277. Appendix B by R. İnanç Baykur. MR2469519 (2009k:57043)

[W1] Jonathan Williams, *The h-principle for broken Lefschetz fibrations*, Geom. Topol. **14** (2010), no. 2, 1015–1061, DOI 10.2140/gt.2010.14.1015. MR2629899 (2011d:57066)

[W2] ———, *The topology of surface diagrams* (2011), available at `http://arxiv.org/abs/1103.6263`.

Max-Planck-Institute for Mathematics, Bonn, Germany